Global Change Biology

WILEY

Global Change Biology

REVIEW

A Theoretical Framework to Quantify Ecosystem Pressure-Volume Relationships

Oliver Binks[1] | Patrick Meir[2] | Alexandra G. Konings[3] | Lucas Cernusak[4] | Bradley O. Christoffersen[5] | William R. L. Anderegg[6,7] | Jeffrey Wood[8] | Lawren Sack[9] | Jordi Martinez-Vilalta[1,10] | Maurizio Mencuccini[1,11]

[1]CREAF, Cerdanyola del Vallès, Barcelona, Spain | [2]School of Geosciences, University of Edinburgh, Edinburgh, UK | [3]Stanford University, Stanford, California, USA | [4]College of Science and Engineering, James Cook University, Cairns, Queensland, Australia | [5]School of Integrative Biological and Chemical Sciences, University of Texas Rio Grande Valley, Edinburg, USA | [6]School of Biological Sciences, University of Utah, Salt Lake City, Utah, USA | [7]Wilkes Center for Climate Science and Policy, University of Utah, Salt Lake City, Utah, USA | [8]University of Missouri, Columbia, Missouri, USA | [9]University of California, Los Angeles, California, USA | [10]Universitat Autònoma de Barcelona, Barcelona, Spain | [11]Institució Catalana de Recerca i Estudis Avançats (ICREA), Barcelona, Spain

Correspondence: Oliver Binks (ojbinks@gmail.com)

Received: 4 April 2024 | **Revised:** 30 September 2024 | **Accepted:** 6 October 2024

Funding: This work was supported by Royal Society (RSWF\211008), Agència de Gestió d'Ajuts Universitaris i de Recerca (BP2021 00224), 'la Caixa' Foundation (LCF/BQ/PI23/11970013), HORIZON EUROPE Climate, Energy and Mobility (862221), Natural Environment Research Council (NE/W006308/1), Australian Research Council (DP17010409).

Keywords: ecohydrological equilibrium theory | ecosystem function | ecosystem water potential | forest water content | moisture release curves | tree hydraulics

ABSTRACT

'Water potential' is the biophysically relevant measure of water status in vegetation relating to stomatal, canopy and hydraulic conductance, as well as mortality thresholds; yet, this cannot be directly related to measured and modelled fluxes of water at plot- to landscape-scale without understanding its relationship with 'water content'. The capacity for detecting vegetation water content via microwave remote sensing further increases the need to understand the link between water content and ecosystem function. In this review, we explore how the fundamental measures of water status, water potential and water content are linked at ecosystem-scale drawing on the existing theory of pressure-volume (PV) relationships. We define and evaluate the concept and limitations of applying PV relationships to ecosystems where the quantity of water can vary on short timescales with respect to plant water status, and over longer timescales and over larger areas due to structural changes in vegetation. As a proof of concept, plot-scale aboveground vegetation PV curves were generated from equilibrium (e.g., predawn) water potentials and water content of the above ground biomass of nine plots, including tropical rainforest, savanna, temperate forest, and a long-term Amazonian rainforest drought experiment. Initial findings suggest that the stored water and ecosystem capacitance scale linearly with biomass across diverse systems, while the relative values of ecosystem hydraulic capacitance and physiologically accessible water storage do not vary systematically with biomass. The bottom-up scaling approach to ecosystem water relations identified the need to characterise the distribution of water potentials within a community and also revealed the relevance of community-level plant tissue fractions to ecosystem water relations. We believe that this theory will be instrumental in linking our detailed understanding of biophysical processes at tissue-scale to the scale at which land surface models operate and at which tower-based, airborne and satellite remote sensing can provide information.

1 | Introduction

Water fluxes from the land surface to the atmosphere deplete pools of water stored in vegetation and soil. These fluxes are mediated by water potential (Ψ), which directly determines hydraulic conductivity in soil (van Genuchten 1980), and is a central physiological variable in plants mediating stomatal conductance (Brodribb and Holbrook 2003; Henry et al. 2019), hydraulic conductance and mortality thresholds associated with water stress (McDowell et al. 2022; Tyree and Sperry 1989). Characterising the feedbacks between stores and fluxes of water, e.g., water content and transpiration, requires relating water content (θ) to Ψ—subsequently referred to as pressure-volume curves (PV curves) for both soil and plants. While PV curves tend to be carried out on small samples (i.e., leaves, stems or ex-situ soil samples), there is mounting interest in understanding how these relationships function at the scale at which land surface models operate, and at which tower-based, airborne and satellite remote sensing can provide information (Konings et al. 2021). Bridging the gap between tissue-level physiological variables and ecosystem-level processes (i) creates the potential for identifying and characterising large-scale vegetation thresholds (Hartmann et al. 2018) and interactions with climate (Anderegg et al. 2019), while (ii) generating a biophysically robust basis for interpreting remote sensing data (Konings, Rao, and Steele-Dunne 2019). In this review, we address the process of scaling plant water relations from tissue to ecosystem by linking sample-scale properties to emergent ecosystem form and function.

In PV curves, water volume is typically expressed as an intensive variable (a property whose magnitude is independent of the size of the system, Box 1), either per volume of medium (plant tissue, soil) or relative to a maximum value. Both Ψ and θ being intensive, the PV relationship is scale invariant where the implicit assumption is that the medium is structurally/biologically homogeneous. Applying it at larger scales, however, inevitably includes varying proportions of media (e.g., leaves, sapwood and heartwood) with distinct PV relationships. In this respect, the volume (an extensive property) and specific part of the system of interest influence the emergent PV relationship. Additionally, a higher volume system has a smaller change in relative water content per unit water loss, indicating the functional value of size to ecosystem water relations. Therefore, linking fluxes to PV states requires an understanding of the total volume of water in the system, i.e., linking intensive with extensive properties. Here, we distinguish the intensive variable 'water content' θ, which can be applied to any part of the system, from the extensive volume of stored water, S, which scales with the total volume (or biomass) of the ecosystem. The volume of stored water in a system changes due to both water stress over short timescales and with biomass over longer timescales in response environmental change. Consequently, biomass, water volume and water potential of ecosystems are fundamentally linked and determine the feedbacks between vegetation and climate.

BOX 1 | Intensive and extensive properties.

"An intensive quantity is one whose magnitude is independent of the size of the system", for example pressure and temperature. Whereas "an extensive quantity is one whose magnitude is additive for subsystems", e.g., volume and mass (Mc Naught and Wilkinson 1997, IUPAC Gold Book). Plant physiologists and soil scientists commonly express quantities of water intensively by making water volume relative to a maximum value or by normalizing by the spatial extent of the system. This is a convenient way of isolating the properties of the system from the environment and provides insight into their internal structure and function. However, 'reconnecting' the system to the environment requires expressing quantities extensively such that a finite input/output results in a quantifiable change in the system. Thus, the intensive property θ (water content, $m^3_{water}\ m^{-3}_{media}$) becomes an extensive volume of water S (m^3) when multiplied by the extensive volume of the system V (m^3).

The concept that plant communities tend towards steady-states of biomass with respect to the supply and demand of water in the system (e.g., the hydraulic environment) and biophysical limitations of plant function is consistent with predictable biogeographical patterns in global biome distribution (Holdridge 1947; Humboldt and Bonpland 1805). Several theories take a probabilistic approach to ecosystem organisation, including Eagleson's ecohydrological equilibrium theory (Eagleson 1982) and maximum entropy production theory (Kleidon, Malhi, and Cox 2010; Kleidon and Schymanski 2008). In both, ecosystems are proposed to converge on optimal solutions with respect to community-level properties (e.g., biomass, water storage, leaf area index). Indeed, multiple plant- to stand-scale vegetation models use steady-state traits to predict longer-term vegetation responses (Cabon et al. 2018; Dewar et al. 2009; Sperry et al. 2019; Yang et al. 2018) over, e.g., decadal timescales, thereby reducing the need to model sub-daily vegetation-climate feedbacks (Franklin et al. 2020). A complementary approach to modelling fluxes in process-based models could be to model steady-states of ecosystem water potential (Ψ_E) and water volume (S_E) in response to the longer-term average conditions, i.e., a 'state-based' modelling approach, relating to the thermodynamic concept of a state function. Potential advantages of a state-based approach include lower data requirements, more clearly defined thresholds for system change (Martinez-Vilalta et al. 2019) and the potential to incorporate longer-term vegetation responses such as acclimation in biochemical processes, adaptation in resource allocation and changes in allometry (Binks et al. 2023; Franklin et al. 2020).

Ecosystem water content, S_E, is also central to the interpretation of microwave and other (e.g., hyperspectral) remote sensing data as a tool for monitoring ecosystem function. Microwave remote sensing measures the dielectric constant of the land surface, which is principally determined by the water contained in biomass, and yields a parameter known as vegetation optical depth (VOD) (Jackson and Schmugge 1991; Konings et al. 2016). However, the interpretation of VOD is currently hampered by a lack of information on the amount of water contained in vegetation, and how vegetation water content links to water potential at ecosystem scale (Konings et al. 2021). The potential for using VOD to monitor ecosystem function and health, therefore, requires an understanding of S_E and ecosystem-level relationships between S_E and Ψ_E.

This article will review the concept of the ecosystem PV curve and its possible applications, theoretical and practical. While the

PV curve has been applied to many different media, ecosystems differ notably in scale, spatial heterogeneity and temporal variability. Therefore, we will open the discussion on the applicability of the PV curve to the ecosystem, referring to fundamental physical concepts described more fully in text boxes. We review the theoretical basis for deriving a single value for ecosystem water potential and water volume, together with practical aspects pertaining to measurement in the field and use of existing data. We also estimate ecosystem and vegetation PV curves for nine sites representative of different biomes and derive some preliminary conclusions, based on established theory and existing data.

2 | Pressure-Volume Theory and Application

There are some key challenges with scaling PV relationships to large, heterogeneous systems with no clear boundary and that are open to continuous exchanges of mass and energy. In this section, we provide some background on water potential and how a concept from equilibrium thermodynamics might be applied to ecosystems. We separate the ecosystems into relevant pools of water and discuss how each pool may contribute to the ecosystem PV relationship. Finally, we present a set of equations describing how each component contributes to ecosystem water relations.

2.1 | Water Potential and Equilibrium Systems

Water potential is a measure of free energy, or chemical potential energy, of water and as such the relationship between water potential and water content is of interest in a variety of contexts and media, e.g., leaves (Tyree and Hammel 1972), wood (Meinzer et al. 2003), rocks (Franzen and Mirwald 2004), soil (Brooks and Corey 1964), even food (Andrade, Lemus, and Pérez 2011) and fabrics (Svennberg and Wadsö 2008) – see Box 3 for a Summary of Water Potential in the Environment. The product of water potential and volume (here $\Psi \cdot S$) represents the difference in the potential energy available to perform work from the same volume of pure water (Gibbs 1873) and is therefore of fundamental importance in biological processes.

In other, smaller-than-ecosystem media, PV parameters tend to be measured under equilibrium conditions, i.e., the absence of gradients in water potential (Box 2). If an ecosystem were to achieve a perfect equilibrium state, Ψ_E would be close to zero at every point within the vertical profile (differing only by gravitation potential) and horizontally across the land surface. This would occur due to capillary rise and vapour transport of water (Rao and Rekapalli 2020) from the water table and horizontal redistribution throughout the soil profile, resulting in full hydration of the plant community. In reality, under conditions of limiting moisture availability arising from evapotranspiration, low soil hydraulic conductance prevents the efficient redistribution of water at sub-seasonal timescales, leading to gradients of Ψ through the soil profile and, therefore, non-saturated ecosystems by definition cannot be at equilibrium. Thus, having established that ecosystems are non-equilibrium systems open to the exchange of mass and energy, the questions arise of how to establish the boundary of an ecosystem, and under what state estimates of system water potential and water volume can reasonably be made.

BOX 2 | Equilibrium and Steady State.

'Equilibrium' refers to the thermodynamic concept of a system at maximum entropy, where energy gradients have dissipated and there are no net fluxes. While evaporation is minimal, the system tends to a state in which the sum of water potential (Ψ) and gravitational potential at any point along the vertical profile is equal to the water potential of the source of water, i.e., there is no net gradient in the sum of energy potentials. Therefore, when transpiration is zero and the vegetation is at maximum possible hydration given the available soil water, the system is at equilibrium. This differs from 'steady-state', which refers to a constant gradient and/or constant flux.

PV curves of leaves (Tyree and Hammel 1972), water retention curves of soil (van Genuchten 1980) and moisture sorption isotherms of porous media (Franzen and Mirwald 2004) are all generated under equilibrium conditions, as gradients in water potential may result in mischaracterising the PV relationship. However, an equilibrium value for a given value of Ψ and water content (θ) may still be approximated in the presence of a Ψ gradient, providing the gradient and the material properties of the medium are sufficiently well characterised (e.g., Figure S1). This could be achieved under steady-state conditions where the gradient is constant, or is changing slowly, over time. For example, it may be possible to know the relevant soil and canopy water potentials of a transpiring tree, but the Ψ and therefore θ at each point in the stem is unknown. In contrast, under 'equilibrium' conditions where the Ψ of the canopy and soil differ only by the difference in gravitational potential, the Ψ is known at each height in the stem, and the θ can be applied based on the known PV curve parameters.

2.2 | Defining Ecosystem Water Potential, Ψ_E

One necessary initial step is to establish the extent of the system, in particular: how deep is an ecosystem? The water table is hydraulically continuous with water in the upper layers of soil and vegetation (Rao and Rekapalli 2020), and the hydraulic conditions below the water table are characterised by the presence of free water ($\Psi \geq 0$ according to depth) across all ecosystems. Ecosystems, therefore, become hydraulically distinct from the water table upwards, making the water table a useful reference point (Binks et al. 2021).

The challenge of representing a system out of hydraulic equilibrium is in characterising the distribution of both water potential and content, which may vary significantly over small temporal and spatial scales, especially during periods of high flux (Figure 1, (Christoffersen et al. 2016)). Assuming comprehensive knowledge of the system, one approach might be to volumetrically weight Ψ between the canopy and water table. Yet, as almost all ecosystem water is contained in the soil (Figure 1e), this would weight Ψ in favour of the part of the system that is least dynamic and least representative of plant

BOX 3 | Summary of Water Potential in the Environment.

Chemical processes, including phase changes and diffusion, progress towards an equilibrium state in which gradients in chemical potential are fully dissipated (Gibbs 1873). The hydrological cycle results from the continuous movement of water down a gradient of water potential towards an equilibrium state and is perpetuated by the spatially and temporally variable input of energy across the Earth's surface (Kleidon and Schymanski 2008; Konings et al. 2012).

Following the pathway of water vertically upwards from its lowest point in a terrestrial system, we can define the water potential (Ψ) of the water table as 0 MPa, being free water at atmospheric pressure and assuming the osmotic potential is negligible. Above the water table, water is bound to the surface of soil particles and in pore spaces via capillarity, where the force of gravity, surface tension acting on menisci, and the resistance to the movement of water generates tension on the water column referred to as matric potential (negative hydrostatic pressure) (Hillel 1977). The relationship between water content of the soil and Ψ is determined by the pore size distribution whereby larger pores empty initially at pressures closer to 0 Pa, while the smallest pores can retain water at substantially lower pressures (Hollander 1979).

In plants, the relationship is more complex where adjacent tissues can maintain Ψ equilibrium by balancing osmotic potential and hydrostatic pressure. In the xylem and in cell walls, pressure is the dominant determinant of water potential (referred to as tension in xylem and matric potential in cell walls), and osmotic potential contributes minimally. In living tissues, water potential is determined by a combination of osmotic potential and turgor pressure (Pickard 1981).

The interface of the liquid-vapour phase change, in vegetation or soil, is typically the point of the system in which liquid water has its lowest chemical potential during evaporation. Evaporation and condensation are driven by the difference in chemical potential between the liquid and vapour (Ambaum 2020). The evaporation of water reduces the hydrostatic pressure, thus Ψ, of the evaporative surface, and the resulting gradient in Ψ is transmitted through the vegetation and/or soil to the point at which Ψ is at its least negative value along the monotonic gradient of Ψ (Nobel 2009; Pickard 1981).

water stress. Furthermore, because the relationship between water potential and content can be strongly non-linear, Jensen's Inequality applies, where the mean of function(x) is not equal to the function of mean(x) (Ruel and Ayres 1999); as a result, the volume-weighted mean water potential is not equal to the equilibrium water potential (Data S1. *A comparison of equilibrium and volume-weighted water potential*).

Although a moisture-limited ecosystem is not at equilibrium, individual non-transpiring plants can theoretically approach hydraulic equilibrium under any prevailing conditions (e.g., Figure 1a,c), either through equilibration with the soil or hydraulic discontinuity between the soil and the roots (Faiz and Weatherley 1982; Rodriguez-Dominguez and Brodribb 2020). In the latter case, the system at equilibrium then becomes the individual plant, which is functionally separated from the soil by a zone of extremely low hydraulic conductance between the soil and roots. Thus, vegetation tends towards a state of hydraulic equilibrium at night in the absence of nocturnal transpiration (Donovan, Richards, and Linton 2003) driven by negative atmospheric water potentials, and during drought when stomatal conductance, and therefore transpiration, is minimal (Mallick et al. 2016; Zeri et al. 2014). As drought progresses, the difference between midday and predawn water potential decreases, indicating minimal flux rates, and it is under these conditions that drought-induced mortality and canopy die-back tend to occur (Martínez-Vilalta and Garcia-Forner 2017), i.e., systems approaching thresholds are typically close to equilibrium water potentials. However, adjacent trees can tend towards different equilibrium water potentials due to variation in rooting depths and the presence of gradients in soil water potential (Sanchez-Martinez et al. 2020), leading to horizontal spatial heterogeneity of equilibrium water potentials across plants. Consequently, the average equilibrium water potential across multiple trees effectively relates to biomass water potential down to a representative community-level rooting depth or functional rooting depth (Binks et al. 2021), i.e., the uppermost soil depth at which a plant is hydraulically equilibrated (Donovan, Richards, and Linton 2003). Thus, a horizontal spatial average of equilibrium/predawn water potentials in individual plants would provide a value of water potential that is reasonably representative of both the above ground biomass, and the average soil depth to which the vegetation is equilibrated (Figure 1). Vegetation equilibrium water potentials may therefore be a suitable proxy for ecosystem water potential.

2.3 | Defining Ecosystem Water Volume, S_E

The scaling of water content θ to an extensive volume S presents the challenge that θ is a property of the medium, not the system, that is, it does not equilibrate. Therefore, even at water potential equilibrium, adjacent media, for example, leaves, wood and soil, may have very different θ.

The amount of water contained in the soil environment (S_{soil}) is around one to two orders of magnitude higher than in vegetation on a ground-area basis (Figure 1e). Consequently, the temporal variation of water stored in the upper fraction of a forest canopy is highly dynamic but of low magnitude, while the amount of water stored in soil layers close to the water table varies over longer time scales and is quantitatively substantial. The remainder of this section focusses on the water content of above ground biomass, S_{AGB}, while S_{soil} is discussed more fully in the Section 2.4.

Characterising the equilibrium PV relationships in a whole tree requires consideration of the roots, heartwood, sapwood, bark and leaves. Roots play a key role in ecosystem hydraulics, substantially mediating the conductance of water between the soil and canopy (Rodriguez-Dominguez and Brodribb 2020; Sperry, Stiller, and Hacke 2003; Steudle 2000), whilst typically having different PV characteristics than either leaves or soil (Aritsara et al. 2022; Bartlett et al. 2022). Root structure (including biomass) and function, however, is very difficult to characterise, while root water relations also remain poorly understood. Therefore, more data are required to address the contribution of root water relations to ecosystems.

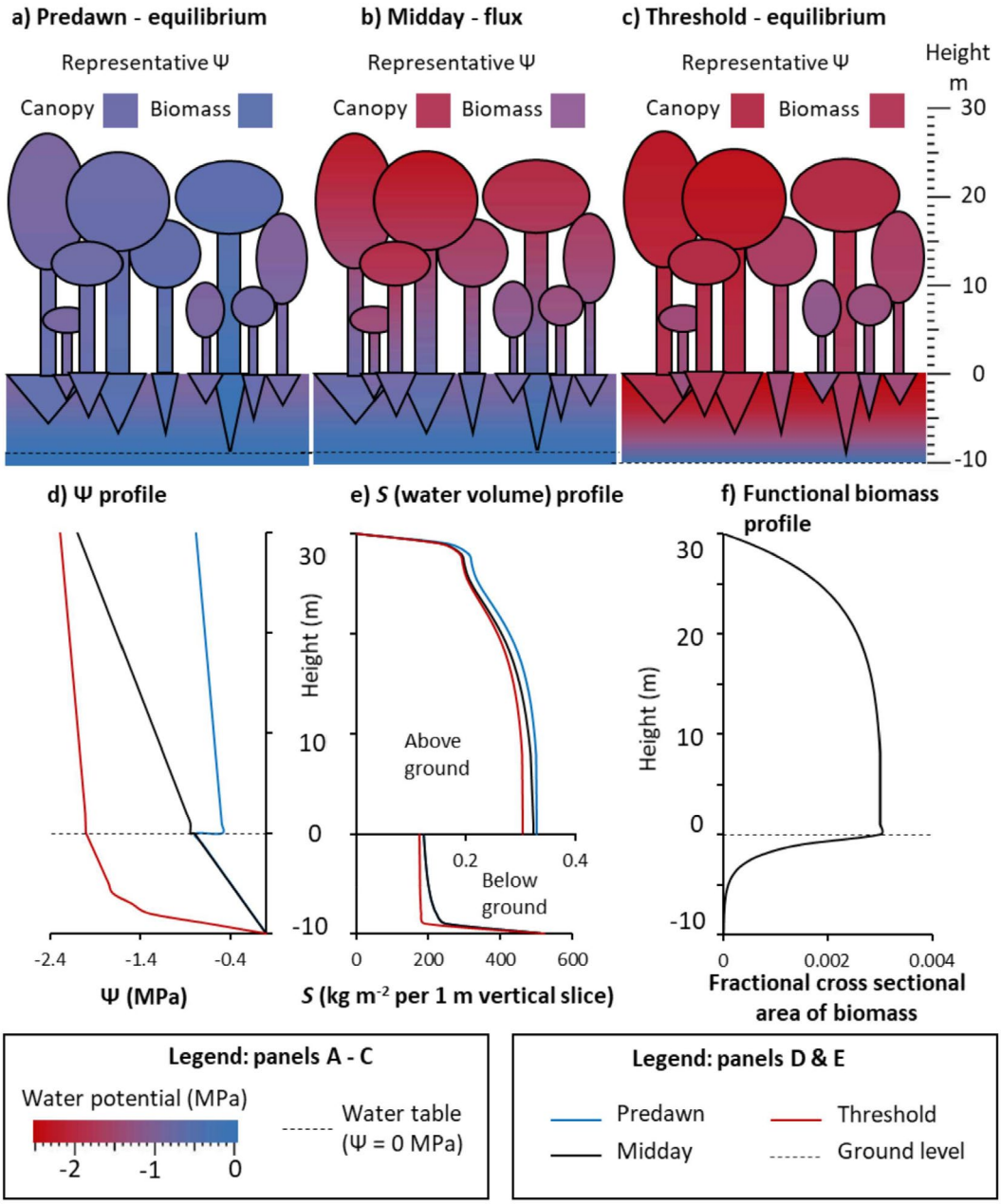

FIGURE 1 | A schematic representing the distributions of water potential (Ψ), water storage (*S*) and biomass, throughout a forest profile. Panels A to C represent predawn non-drought (a); midday non-drought (b); and drought (c). The square boxes indicate 'representative' water potentials of the canopy and biomass in each scenario (where the colours relate to the water potential scale in the legend), i.e., the Ψ value of leaves at the top of the canopy, and a value intermediate between upper leaves and roots—these values converge at equilibrium. Panel (d) indicates the vertical profile of Ψ. Panel (e) represents the profile of water stored per ground area such that, for each horizontal slice (of 1 m vertical thickness), the water content is weighted by the biomass density given in (f) – note the different x axis applying to above and below ground fractions, and that $1\,kg_{water}\,m^{-2}{}_{ground\ area} = 1\,mm$ water thickness $= 10\,Mg_{water}\,ha^{-1}$. Panel (f) shows a profile of the fraction of woody cross sectional area ($m^2{}_{biomass}\,m^{-2}{}_{ground\ area}$) of a notional temperate forest. All gradients in Ψ are linear for simplicity (panel d), but this is unlikely to be representative of real conditions.

The current consensus is that the water contained in heartwood, which comprises 40%–60% of wood volume in mature trees (Čermák et al. 2007; Cordero and Kanninen 2003; Knapic, Tavares, and Pereira 2006; van der Sande, Zuidema, and Sterck 2015), does not contribute substantially to plant hydraulic function (Holbrook Gartner 1995; Venturas, Sperry, and Hacke 2017). However, the consideration of heartwood water, S_{hw}, also depends on the extent to which it can be detected by microwave remote sensing signals. Low frequency signals (e.g., L-band) can penetrate through dense canopy to ground-level (Brandt et al. 2018; Frappart et al. 2020). While this is not evidence in of itself that signals penetrate the inner tissues of tree stems, some field-based studies indicate L-band woody tissue penetration depths of 5–10 cm (Koubaa et al. 2008; Mavrovic et al. 2018; Ulaby and Long 2014), providing an estimate of the maximum likely sensing depth of satellite signals. Thus, it may be necessary to consider the total heartwood water to serve as an upper limit on the estimate of total above ground water content.

Sapwood contains a physiologically and quantitatively important store of water (S_{sw}) at ecosystem level, while water stored in leaves (S_{leaves}) may be small in proportion to S_{sw} in high biomass systems but likely contributes significantly to daily transpiration fluxes. Moreover, S_{leaves} may have a disproportionate effect on the VOD signal from microwave remote sensing applications (Holtzman et al. 2021). Therefore, sapwood and canopy water content comprise the physiologically active and temporally variable store of water in above ground biomass, and we refer to this as the 'dynamic' water, S_D.

2.4 | Soil Water

The volume of water stored in soil is a function of soil depth, $S_{soil}(D_x)$. Selecting a representative soil depth (D_x) requires consideration of the challenges in characterising gradients in Ψ and θ, representation over time and the possibility for the comparison between different ecosystems.

Three possibilities for standardising soil depth across systems are: (i) water table depth; (ii) the rooting depth as determined by predawn water potentials in conjunction with known soil water potential profiles (i.e., the 'functional rooting depth'); and (iii) zero depth, i.e., excluding the soil component. The first two options vary spatially and temporally and are rarely known with a high degree of certainty. The final option avoids the problem of 'drowning' out the signal from the plants, is easy to standardise across sites, is effectively equal to the functional rooting depth at soil saturation (i.e., $\Psi_{soil} = 0$) and selects the fraction of the system relating to above ground biomass, which is relatively well characterised. See Data S2. *Soil Depth* for further discussion of the limitations to characterising S_{soil}.

For those reasons, we define ecosystem water content, S_E, as including a soil fraction to depth D_x for the sake of providing a complete theory. However, in our *Proof of Concept* we address the water contained in above ground biomass only (S_{AGB}) in the main text, but include the calculation of S_E for a single site in Data S3.

2.5 | Ecosystem Pressure-Volume Curves: Combining the Components

Following the previous discussion, we may treat the ecosystem as having four relevant components, where the total amount of water stored in the ecosystem (S_E) is partitioned between the leaf area (S_{leaves}), sapwood (S_{sw}), heartwood (S_{hw}) and soil (S_{soil}), where each component is a quantity of water normalised by ground area, e.g., kg m^{-2} or equivalently mm. With the exception of S_{hw}, which may remain constant, each component potentially has a unique PV relationship. Because we are considering a system at equilibrium, these components all have the same water potential (Ψ_{eq}), and therefore, the ecosystem PV curve becomes the sum of the water from each component at each value of equilibrium water potential over a given range.

$$S_E(\Psi_{eq}) = S_{leaves}(\Psi_{eq}) + S_{sw}(\Psi_{eq}) + S_{hw} + S_{soil}(\Psi_{eq}) \quad (1a)$$

For the purpose of analysis and interpretation it is useful to subdivide S_E into the water stored in the above ground biomass only:

$$S_{AGB}(\Psi_{eq}) = S_{leaves}(\Psi_{eq}) + S_{sw}(\Psi_{eq}) + S_{hw} \quad (1b)$$

And into the above ground components relating to plant water status, that is, the dynamic stored water:

$$S_D(\Psi_{eq}) = S_{leaves}(\Psi_{eq}) + S_{sw}(\Psi_{eq}) \quad (1c)$$

The water contained in each component is the product of its volume V (m^3) and water content θ ($m^3\,m^{-3}$) as a function of Ψ, which we express per ground area as total water thickness (mm):

$$S_{soil}(\Psi) = \rho_{water} \bullet D \bullet \theta_{soil}(\Psi) \quad (2)$$

$$S_{sw/hw}(\Psi) = \rho_{water}\left[\sum_{tree=1}^{n} V_{sw/hw\_tree} \bullet \theta_{sw/hw\_tree}(\Psi) / A_{plot}\right] \quad (3)$$

$$S_{leaves}(\Psi) = LAI \bullet \theta_{leaf}(\Psi) \quad (4)$$

Where D (m) is soil depth (Equation 2); V_{sw/hw_tree} is the volume of sapwood or heartwood per tree (noting that θ_{hw} in this analysis does not change with Ψ) in a plot of area A_{plot} (m^2) with n trees (Equation 3); LAI ($m^2_{leaf\_area}\,m^{-2}_{ground\_area}$) is the leaf area index, and leaf water content (θ_{leaf}) is expressed per one-sided leaf area ($kg\,m^{-2}$, Equation 4). For practical purposes, the 'leaves' fraction (Equation 4) does not separate leaf area into individual trees as this information is rarely known, but instead uses a value for θ_{leaf} that represents a stand average.

Scaling sapwood and heartwood water content $\theta_{sw/hw}$ to tree-level requires their respective volumes per tree.

$$V_{sw\_tree} = \frac{AGB_{tree}F_{sw\_tree}}{\rho_{wood\_tree}} = V_{tree}F_{sw\_tree} \quad (5a)$$

$$V_{hw\_tree} = V_{tree} - V_{sw\_tree} \quad (5b)$$

Where the subscript '*tree*' denotes individual tree-level values, *AGB* is the above ground biomass (kg), ρ_{wood} is wood density ($kg\,m^{-3}$) and F_{sw} is the volume fraction of sapwood (see Data S4 *Deriving the sapwood fraction*, F_{sw}).

Soil, sapwood and leaves have different PV curves determining θ (Ψ), where the slope of dθ/dΨ is referred to as hydraulic capacitance. Various equations have been derived to model the PV relationship in soils (see Data S1 for a typical example (van Genuchten 1980)). In both leaves and sapwood, PV curves tend to have a linear region of constant hydraulic capacitance at higher values of Ψ (Bartlett, Scoffoni, and Sack 2012; Carrasco et al. 2015; Meinzer et al. 2003; Scholz et al. 2007; Tyree and Ewers 1991; Wolfe and Kursar 2015; Ziemińska et al. 2020), which in sapwood is typically expressed intensively (C_{sw}, $kg\,m^{-3}\,MPa^{-1}$), while in leaves it

is often expressed per leaf area ($kg\,m^{-2}\,MPa^{-1}$). Following the linear region of capacitance in leaves and sapwood, they then rapidly lose water in a post-threshold phase in which capacitance declines exponentially towards 0. The relationship between θ and Ψ can therefore be modelled in two phases ('leaves or sapwood' denoted as 'l/sw'):

$$\theta_{l/sw}(\Psi_i) = \begin{cases} \theta_{l/sw}(\Psi_0) - C_{l/sw}[\Psi_0 - \Psi] & \Psi \geq \Psi_{threshold} \\ \theta_{l/sw}(\Psi_{threshold}) \bullet \left([\Psi_0 - \Psi_{threshold}]/[\Psi_0 - \Psi]\right) & \Psi < \Psi_{threshold} \end{cases} \quad (6)$$

where subscripts 0 and *threshold* indicate the corresponding water potentials, and C is the (constant) intensive hydraulic capacitance (Box 1) of the linear proportion of the curve. Figure 2a illustrates the shapes of the curves and their parameters. The '$\Psi_{threshold}/[\Psi_0\text{-}\Psi]$' term in Equation 6 is based on a more general form of Equation 3 in Christoffersen et al. (2016) describing the post-threshold part of the leaf PV curve. See Data S5 *Deriving post-threshold capacitance in leaves and sapwood*.

3 | Proof of Concept

Here we explore the relationship between Ψ and S at large scale using plot-level PV curves of the above ground biomass from nine sites representing tropical rainforest, temperate forest, tropical savanna and semi-arid savanna (Data S6, Table S6.1). The sites were chosen to represent a broad range of biomass, and climates, and based on available data. We address each pool of water in turn discussing practical ways of using existing data to best represent the theory generated above. See Table 1 for the descriptions and equations describing each of the variables in the derivation. Values of θ(Ψ) were generated for each component based on a sequence of Ψ from −10 MPa (Ψ_{min}) to 0 (Ψ_0). We omitted the soil component from the main analysis (see Section 2.4), addressing only the components of the above ground biomass, but have illustrated a full ecosystem PV curve including a soil component for one site in Data S3.

3.1 | Canopy PV Curves

Leaf-level PV curves were generated (Equations 4 and 6) from each site largely based on the biome-level parameter values reported in Bartlett, Scoffoni, and Sack (2012) and modelled relationships from Christoffersen et al. (2016). Leaf turgor loss point was used as the threshold value for leaves ($\Psi_{TLP} = \Psi_{threshold}$), marking the transition from the linear to the non-linear phase of the PV relationship (Tyree and Hammel 1972). See Table S6.2 for leaf water relations parameters.

3.2 | Sapwood PV Curves

Sapwood PV curves were generated per tree according to Equations 3, 5a and 6, and plot-level values were calculated from the combined properties of all trees (Figure 2) based on forest inventory data from the sites listed in Table S6.1 (All data are available in a Dryad repository, see Binks et al. 2024). The individual tree-level approach enables the incorporation of random variability of parameters between individuals and species; and allows the addition of individual- or species-specific traits (e.g., wood density) resulting in different values of $\theta(\Psi_i)$.

The Ψ_0 value in Equation 6 was substituted for Ψ_{max} in the sapwood which is the least negative water potential with respect to tree height (Table 1) assuming no foliar water uptake (Binks et al. 2019).

Ideally, the threshold water potential in sapwood, $\Psi_{threshold}$, should represent the most negative Ψ from which plants can

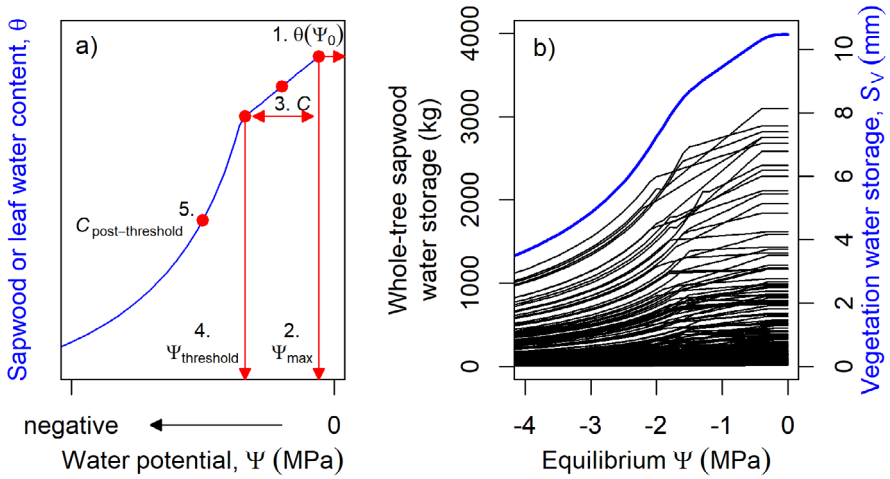

FIGURE 2 | Panel (a) shows a schematic relationship between water content (θ) and water potential (Ψ) of sapwood or leaves, generated using the following parameters: 1. Saturated water content, $\theta(\Psi_0)$; 2. Maximum water potential, Ψ_{max}; 3. Constant hydraulic capacitance throughout 'normal' physiological range indicated by the red double ended arrow, C; 4. Threshold water potential at which the PV relationship transitions into non-linear region, $\Psi_{threshold}$; 5. Exponentially declining capacitance as a function of water potential, $C_{post\text{-}threshold}$. Panel (b) shows modelled relationships between the amount of water stored in the sapwood of individual trees (black lines, left axis) versus their equilibrium water potential in a simulated one hectare stand. The blue line in panel (b) shows the total water stored in the above ground biomass (S_V, right axis) including the sum of all the sapwood water expressed per ground area, with respect to the equilibrium 'ecosystem water potential' (Ψ_E), blue line.

TABLE 1 | Parameters used to derive the pressure-volume curves at the canopy- (plot-level averages), sapwood- and plot-level.

Parameter (units)	Description	Derivation and/or references
Ψ_{max} (MPa)	Maximum (least negative) water potential	H_{tree} x − 0.01, where H_{tree} is tree height (m), and − 0.01 is a constant describing the gravitation effect on pressure (MPa m^{-1}) in a water column.
$\Psi_{predawn}$ (MPa)	Measured predawn canopy water potentials	See Table S1 for sources of data.
$\Psi_{threshold}$ (MPa)	Minimum safe water potential	This value is based on dry season midday leaf water potentials for the purpose of this analysis (See Data S4. *Choosing a threshold water potential*). Each tree was randomly allocated a value for $\Psi_{threshold}$ from a random normal distribution generated from the mean and standard deviation of midday leaf water potential values taken at a given site.
Ψ_{TLP} (MPa)	Leaf turgor loss point	Values taken from Bartlett, Scoffoni, and Sack 2012; Binks et al. 2016; Peters et al. (2021). See Table S3
$S_{leaves}(\Psi_i)$ (mm)	Canopy leaf water	Total water contained in leaf area per ground area at Ψ_i. Equation 4.
$S_{sw}(\Psi_i)$ (mm)	Sapwood water	Total water contained in sapwood per ground area at Ψ_i. Equation 3.
$S_{hw}(\Psi_i)$ (mm)	Heartwood water	Total water contained in heartwood per ground area at Ψ_i. Equation 3.
S_{soil} (mm)	Soil water	Total water contained in soil from the surface to depth *D*. Equation 2.
S_D (mm)	Dynamic vegetation water	Total water contained in the sapwood and canopy per ground area at Ψ_i. $S_D = S_{leaves} + S_{sw}$
S_{AGB} (mm)	Above ground biomass water	Total water contained in the sapwood, canopy and heartwood per ground area at Ψ_i. $S_{AGB} = S_{leaves} + S_{sw} + S_{hw}$
S_{AGB_a} (mm)	Accessible vegetation stored water	The difference in S_{AGB} between Ψ_{max} and the (equilibrium) threshold water potential, i.e., the theoretical maximum change in vegetation seasonal water storage.
S_E (mm)	Ecosystem water content	Total water contained in ecosystem per ground area. $S_E = S_{AGB} + S_{soil}$. Equation 1a.
C_{sw} (kg m^{-3} MPa^{-1})	Sapwood intensive capacitance of the linear phase of the pressure-volume curve.	Where field data exist, each tree was randomly allocated a value for C_1 from a random normal distribution generated from the mean and standard deviation of capacitance values. In the absence of field data, the mean value was derived from an empirical equation from Ziemińska et al. (2020) of the form: $C_{sw} = -157.8 \cdot \rho + 137.7$, where ρ is wood density, and the standard deviation was taken as $0.5C_{sw}$.
C_{leaves} (mm MPa^{-1})	Hydraulic capacitance of leaf area	$C_{leaves} = \left(\frac{LAI \bullet \theta_{leaf}(\Psi_0)[1 - \Theta_{leaf}(\Psi_{TLP})]}{-\Psi_{TLP}} \right)$
C_{AGB} (mm MPa^{-1})	Vegetation hydraulic capacitance	The sum of the plot-level sapwood capacitance and the canopy capacitance. Equation 8.
F_{sw} (dimensionless fraction)	Sapwood as a fraction of total volume	$F_{sw} = 2.9 \cdot DBH^{-0.6}$, derived as a compromise between the empirical relationship presented by Cordero and Kanninen (2003), and the ratio of sapwood area to basal area from Kunert et al. (2017), Moore et al. (2017), Aparecido et al. (2016) and Wang et al. (2009). See S2 for full details on deriving F_{sw}.

(Continues)

TABLE 1 | (Continued)

Parameter (units)	Description	Derivation and/or references
F_{hw} (dimensionless fraction)	Heartwood as a fraction of total volume	$F_{hw} = 1 — F_{sw}$
V_{sw_tree} (m^3)	Volume of sapwood in a single tree	$V_{sw\_tree} = F_{sw} \cdot AGB_{tree}/\rho$
V_{hw_tree} (m^3)	Volume of heartwood in a single tree	$V_{hw\_tree} = F_{hw} \cdot AGB_{tree}/\rho$
$\theta_{leaf}(\Psi_0)$ ($kg\,m^{-2}_{leaf\ area}$)	Leaf saturated water content	Derived from leaf mass per area (LMA) data as per Stewart et al. 1990, except for field site in Caxiuana, Brazil, which were measured by Binks et al. (2016). Plot mean LMA data from non-Caxiuana field sites were estimated from MODIS data (ORNAL DAAC 2018).
$\Theta_{leaf}(\Psi_{TLP})$ (unitless)	Leaf relative water content at turgor loss point	Biome-level values taken from Bartlett, Scoffoni, and Sack 2012, except for field site in Caxiuana, Brazil, which were measured by Binks et al. 2016
$\theta_{sw}(\Psi_0)$ ($kg\,m^{-3}$)	Saturated sapwood water content	An empirical relationship reported by Dlouhá et al. (2018) where $\Theta_{sat\_sw} = -0.67 \cdot \rho + 1$, and ρ is wood density.
ρ_{wood} ($kg\,m^{-3}$)	Wood density	The ratio of dry mass to fresh volume used to derive C_{sw}, Θ_{sat_sw}, and V_{AGB}. Obtained at species-level from plot inventories.
ρ_{water} ($kg\,m^{-3}$)	Water density	$1000\,kg\,m^{-3}$
H_{tree} (m)	Tree height	Available in the datasets.
AGB ($Mg\,ha^{-1}$)	Oven dried above ground biomass	Taken from existing datasets
LAI ($m^2\,m^{-2}$)	Leaf area index	Values taken from Beringer et al. 2016, except for field site in Caxiuana, Brazil, which were measured by Fisher et al. (2006).

recover full hydraulic function without growing new/replacement tissue (Data S7. *Choosing a threshold water potential*). Here, $\Psi_{threshold}$ at plot-level was based on the plot-level mean of the observed dry season midday water potentials (Ψ_{md}). Critically, when the system is at equilibrium *and* the system has dehydrated to the threshold water potential, it follows that the water potential throughout the entire sapwood is also at the threshold water potential (Figure 1c). Thus, when the system is at $\Psi_{threshold}$, the canopy is experiencing a Ψ that occurs within the 'normal' diurnal range, while the majority of the sapwood is experiencing lower than normal water potentials. Individual trees were allocated a value for $\Psi_{threshold}$ taken from a random normal distribution based on the mean and standard error of reported plot-level Ψ_{md} (Table 1).

3.3 | Heartwood Water Content

Because of the sparsity of data on heartwood water content, S_{hw}, the mixed evidence that it is hydraulically coupled with the sapwood (See Section 4.6), and the lack of PV information on heartwood, we have treated heartwood water content as constant, i.e., not changing with water potential. Assuming that there is minimal change over seasonal to annual time scales is a parsimonious approach given the available evidence and data.

We use a mean value for heartwood water content of 0.328 $m^3_{water}\ m^{-3}_{heartwood}$ +/− 0.013 standard error. This was based on data taken from Umebayashi (2011–10 species), Glass & Zelinka (2010–68 species) and combined with unpublished data (13 species) collected from an Amazonian rainforest plot in Caxiuana, Brazil. See Data S8 *Heartwood water content* for details. Heartwood volume was calculated per tree according to Equation 5b.

3.4 | Vegetation Hydraulic Capacitance and Water Storage

Hydraulic capacitance of the plot-level above ground biomass (C_{AGB}, mm MPa^{-1}) was calculated as the sum of tree-level sapwood capacitance (C_{sw_tree}, kg MPa^{-1}) normalised by ground area (A_{plot}, m^2) and canopy capacitance (C_{leaves}, mm MPa^{-1}) in the linear phase of the PV curves:

$$C_{AGB} = \left(\frac{\sum_{tree=1}^{n} \left(C_{sw\_tree} V_{sw\_tree} \right)}{A_{plot}} \right) + \mathrm{LAI} \left(\frac{\theta_{leaf}(\Psi_0)\left[1 - \Theta_{leaf}(\Psi_{TLP})\right]}{-\Psi_{TLP}} \right) \quad (7)$$

Where $\Theta_{leaf}(\Psi_{TLP})$ is the leaf relative water content at turgor loss point ($\theta_{TLP}/\theta_{Saturated}$, Table 1).

'Accessible water' (S_{AGB_a}, mm) was taken to be the difference in S_{AGB} between Ψ_{max} and the (equilibrium) threshold water potential, i.e., the difference in water content in panels A and C in Figure 1.

$$S_{AGB\_a} = S_{AGB}(\Psi_{max}) - S_{AGB}(\Psi_{threshold} + sd) \quad (8)$$

The lower boundary was taken to be $\Psi_{threshold}$ + 1 standard deviation of measured Ψ_{md} (sd) to account for the distribution of $\Psi_{threshold}$ of the individual trees, half of which would be less negative than plot mean $\Psi_{threshold}$.

3.5 | Results of the 'Proof of Concept'

Values relating to the dynamic water storage (sapwood and leaves, S_D) are presented followed by the total above ground water storage (including heartwood, S_{AGB}) in square brackets. The analysis showed a range of $S_D(\Psi_0)$ from 0.2 mm [0.3] in semi-arid savanna to 17.0 mm [33.6] in tropical rainforest (Figures 3 and S6.1). Water in leaves (S_{leaves}) ranged from 19.4% [14.9] to 1.2% [0.5] of $S_D(\Psi_0)$ [$S_{AGB}(\Psi_0)$] in the lowest to highest biomass systems, respectively (Figure 4). The traits relating to extensive quantities of stored water (Figure 5a,c,e,f) were all related to stand biomass (also an extensive quantity), i.e., they scale with system size, including hydraulic capacitance ($p = 0.003$, $r^2 = 0.70$), accessible storage ($p = 0.009$, $r^2 = 0.71$), maximum dynamic water content ($S_D(\Psi_0)$, $p = 0.001$, $r^2 = 0.77$) and the total water stored in above ground biomass ($S_{AGB}(\Psi_0)$, $p << 0.001$, $r^2 = 0.92$). The ratio of $S_D(\Psi_0)$ to biomass was approximately 1:3 (0.31 +/− 0.06 $kg_{water}\ kg_{biomass}^{-1}$, regression slope +/− standard error, Figure 5e) across all sites, and for $S_{AGB}(\Psi_0)$ it was 2:3 (0.66 +/− 0.07 $kg_{water}\ kg_{biomass}^{-1}$, Figure 5f). The $S_D(\Psi_0)$ to biomass relationship was largely driven by sapwood water content, although $\theta_{sw}(\Psi_0)$ was derived from an empirical relationship with wood density (Dlouhá et al. 2018) which differed across sites, and the relationship included low biomass sites with proportionally higher S_{leaves}.

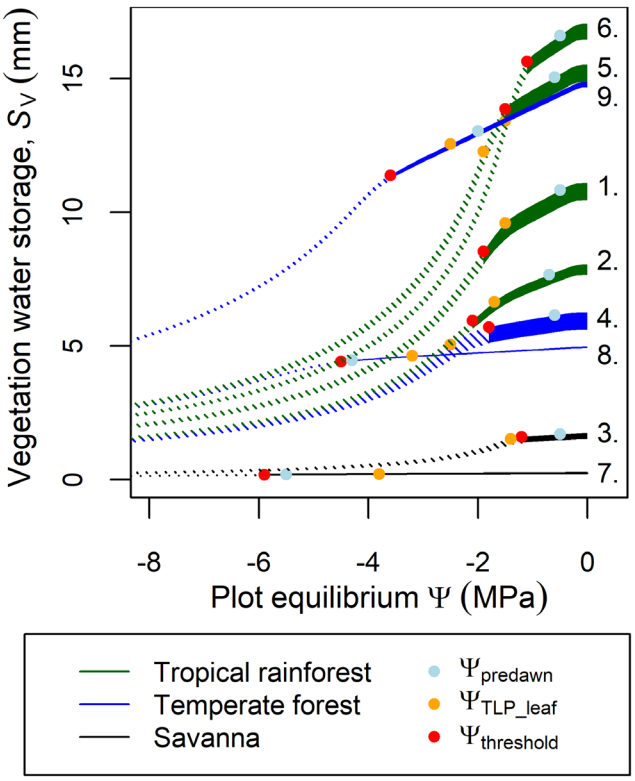

FIGURE 3 | Ground area based dynamic water storage (sapwood + canopy) versus equilibrium water potential of the ecosystems described in Table S2: 1. Caxiuana (non-drought); 2. Caxiuana (artificially droughted); 3. Litchfield; 4. Tumbarumba; 5. Cow Bay; 6. Robson Creek; 7. Alice Mulga (semi-arid savanna); 8. Great Western Woodland; 9. Cumberland Plain. Each 'curve' is constructed from two lines, where the lower line represents the plot-level PV curve of the sapwood, and the upper line is the sum of the water content from sapwood and the canopy/leaf area; so, the difference between the curves, i.e., the line thickness, represents the canopy water content. The filled areas were constructed using data, while the hatched areas represent approximations of the PV relationship at water potentials below the water potential threshold. The points on each curve represent equilibrium water potentials as measured at predawn (blue), threshold, i.e., midday (red), and leaf turgor loss point (orange).

The mean intensive vegetation capacitance was 0.023 +/− 0.003 $kg_{water}\ kg^{-1}_{biomass}\ MPa^{-1}$ across sites. Two relative values of capacitance were derived by normalising by $S_D(\Psi_0)$ (0.069 +/− 0.009 MPa^{-1}) and $S_{AGB}(\Psi_0)$ (0.034 +/− 0.004 MPa^{-1}), but neither of these relativised capacitance values varied systematically with biomass (Figure 5b, Figure S6.2).

According to the thresholds selected in the analysis the relative accessible storage, i.e., the maximum difference in above ground water storage without incurring physiological damage, is around 14.6% +/− 2.4 of $S_D(\Psi_0)$ and 7.4% +/− 1.6 of $S_{AGB}(\Psi_0)$ (Figure 5d, Figure S6.2). The first value, relating to the functionally active tissue, is within the range of empirically derived values of the relative water loss between saturation and the water potential threshold of leaves (i.e., Ψ_{TLP}, (Martinez-Vilalta et al. 2019) and stems (Rosner, Heinze, and Savi 2019)).

4 | Discussion of Ecosystem Pressure-Volume Relationships

The emergent properties arising the from the *Proof of Concept* are used as a basis to discuss the utility and limitations of upscaling plant water relations. The state-based approach to ecosystem water relations is reviewed in the context of generating new perspectives on climate-biomass thresholds and how it relates to remote sensing and modelling at large spatial scales. We also consider how spatial scaling of ecophysiological characteristics may require an alternative approach to sampling vegetation at the plot scale. Finally, we discuss some limitations of the approach and avenues for further research.

4.1 | Thresholds

A key focus of large-scale vegetation ecology is in predicting and detecting thresholds of water stress that lead to significant mortality events or transitions in vegetation type. In sapwood, the transition between the pre- and post-threshold phases of the PV curve is often apparent from a change in the $d\theta/d\Psi$ gradient caused by the release of water from cavitating vessels (Hölttä et al. 2009; M. Tyree and Ewers 1991). It is possible that a similar mechanism of water release occurs at large spatial and time scales. Drought, soil and/or atmospheric, leads to the death of living biomass (leaves, branches, whole plants) causing the amount of 'dynamic' water contained in the system to decrease rapidly, while both the competition for soil water and the soil-atmosphere hydraulic conductance are reduced, slowing the

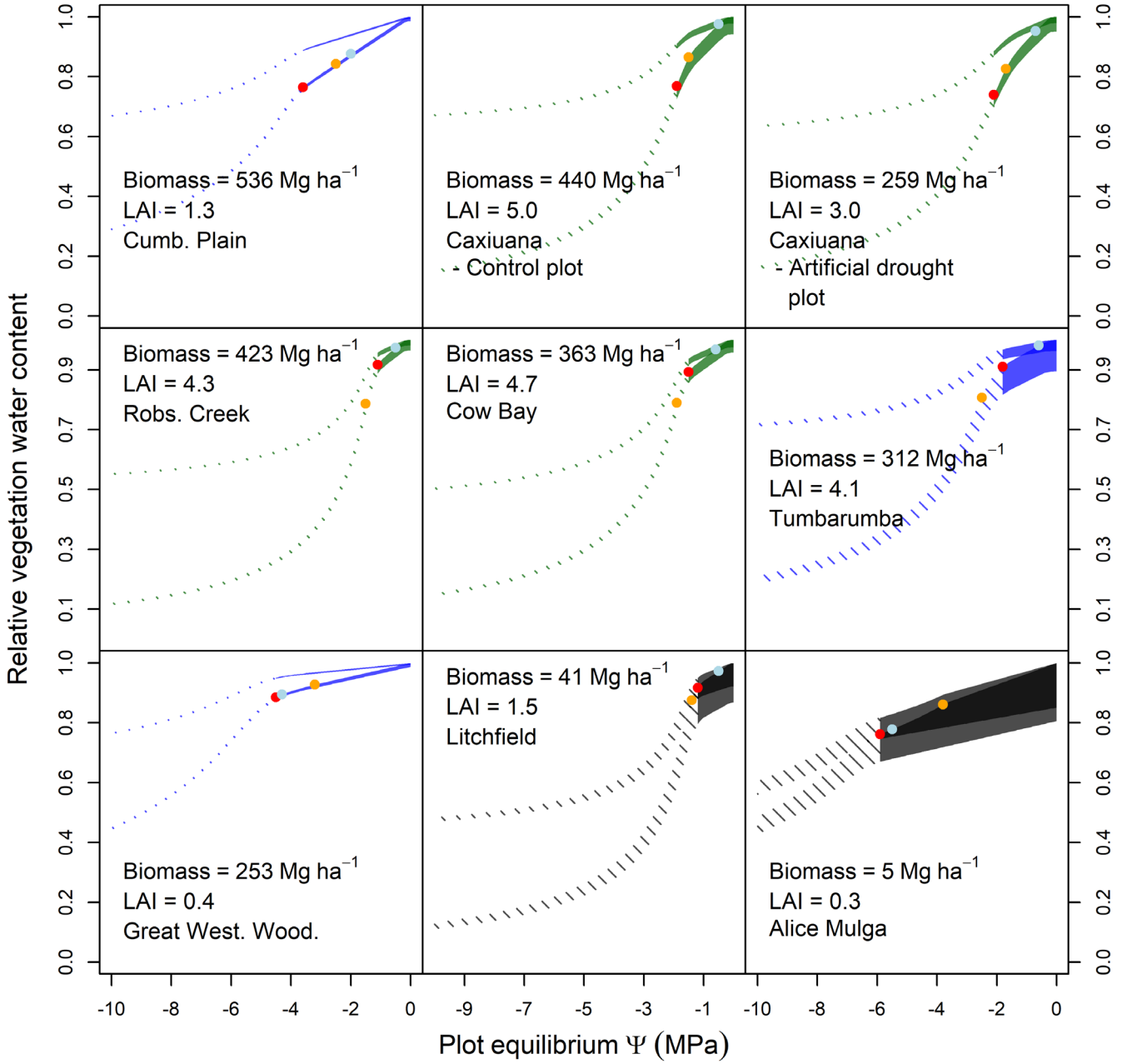

FIGURE 4 | Relative water volume versus water potential of the sites described in Table 1, where the upper curve in each panel is the estimated total above ground water content, including sapwood, heartwood and leaves, and lower curve includes only sapwood and leaves (the 'dynamic' fraction). Each 'curve' is constructed from two lines, where the lower line represents the plot-level PV curve of the wood fraction, and the upper line is the sum of the water content from the wood and the canopy/leaf area; so the difference between the curves, that is, the line thickness, represents the canopy water content. The filled areas were constructed using data, while the hatched areas represent approximations of the PV relationship following the water potential threshold for sapwood. The points on each curve represent equilibrium water potentials (Ψ) as measured at predawn (blue), threshold, that is, midday (red) and leaf turgor loss point (orange).

decline in plant equilibrium water potentials. The ecosystem thus transitions into a phase where the loss of water in above ground biomass, S_{AGB}, happens more rapidly than the corresponding change in water potential, Ψ_{AGB}, and this continues until there is sufficient water for Ψ_{AGB} to be maintained within physiologically tolerable limits in the remaining vegetation.

A central consideration of thresholds at community-level is whether there is an acute transition between the pre- and post-$\Psi_{threshold}$ parts of the EPV curve (Wood et al. 2023). For the purpose of the *Proof of concept*, the post-$\Psi_{threshold}$ PV relationship was based on the shape of published PV curves, by simplifying the derivation of Christoffersen et al. (2016). However, the extent that ecosystems follow the same pattern as plant tissues is unknown, and might only become apparent from large-scale observation and experiments (Mcculloh et al. 2014; Meir et al. 2015). Evidence from the Caxiuana long-term throughfall-exclusion experiment (CTFE) in Amazonian rainforest in Brazil (Meir et al. 2018) suggests that the pre- and post-threshold change in $d\theta/d\Psi$ may be considerable, that is,

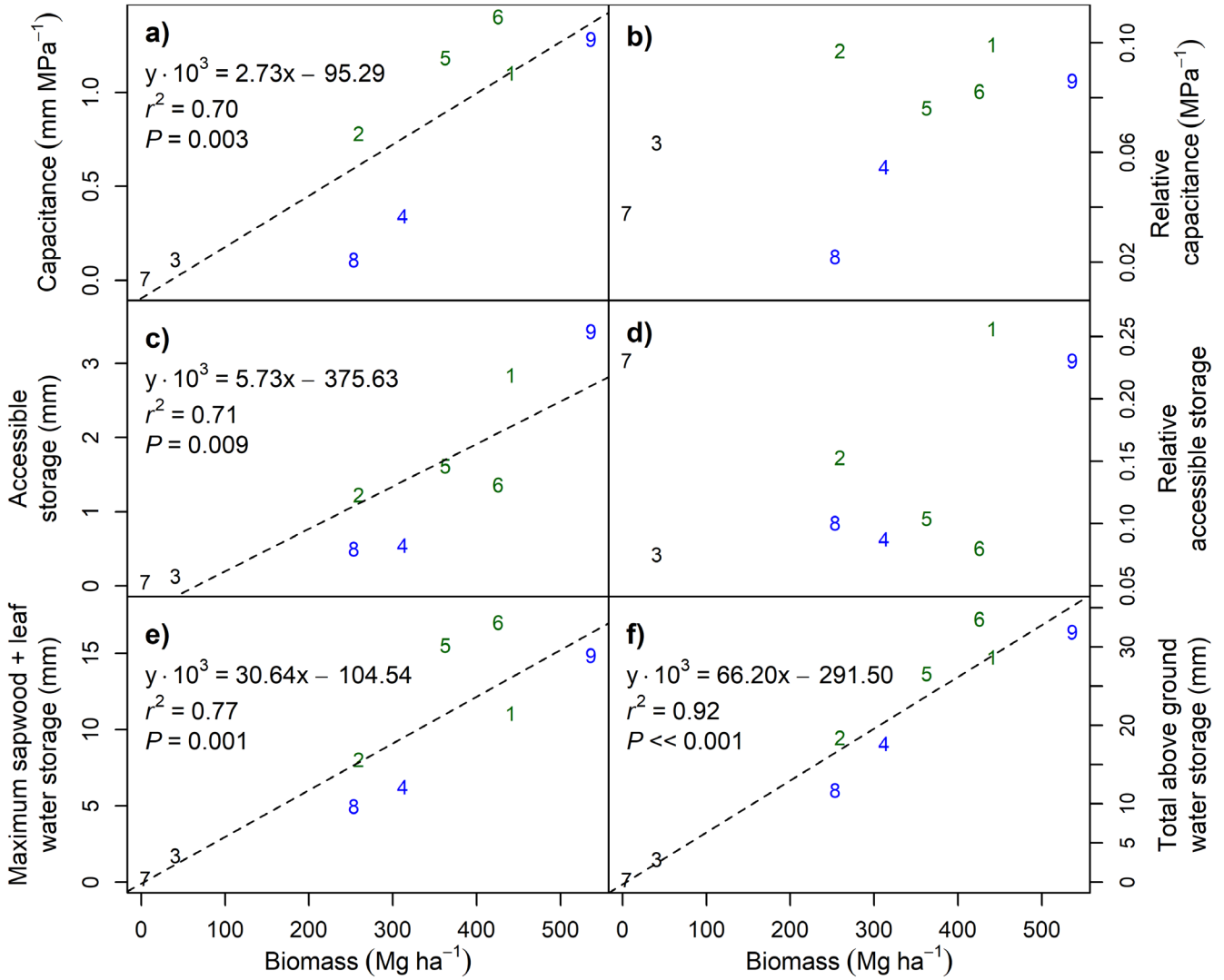

FIGURE 5 | Plot-level water relations parameters in relation to biomass expressed in absolute terms (a, c, e, f) and relative to the maximum water stored in the sapwood and leaves (b, d), i.e., shown in panel e. Hydraulic capacitance (a, b), accessible stored water between the maximum water potential and the threshold water potential (c, d), the amount of water stored in sapwood and leaves at saturation (e), and the total maximum amount of water stored in above ground biomass including the heartwood (f). Each number on the plot represents data from each site described in Table 1, where colours represent tropical rainforest (green), temperate forest (blue) and savanna (black): 1. Caxiuana (non-droughted); 2. Caxiuana (droughted); 3. Litchfield (wet trop. savanna); 4. Tumbarumba; 5. Cow Bay; 6. Robson Creek; 7. Alice Mulga (semi-arid savanna); 8. Great Western Woodland; 9. Cumberland Plain. Linear regressions are shown where the relationships are significant (a, c, e, f), although none of the intercepts differ significantly from 0; the y variable was multiplied by 10^3 to reduce the significant figures of the coefficients. 1 mm of water thickness = 1 kg_{water} $m^{-2}{}_{ground\ area}$ = 10 Mg_{water} ha^{-1}.

the transition from one line to the other in Figure 6. The CTFE excluded 50% of the throughfall from 1 ha of rainforest continuously since 2002, resulting in elevated mortality and lower biomass (da Costa et al. 2010; Yao et al. 2022). The droughted forest now has lower ecosystem water content, while the diurnal range of canopy leaf water potentials remains similar, although slightly more negative, than those in the control (Bittencourt et al. 2020). The opposite effect has also been observed in forest irrigation experiments, where biomass increases but water potentials remain similar (Schönbeck et al. 2018). These experimental results are consistent with the theory presented here: that changes in the hydraulic environment result in co-dependent changes in biomass and S_{AGB} such that the water: biomass ratio is approximately conserved, while maintaining water potentials within the narrow limits required for physiological function (Figure 5e,f).

At community-level, transitions may become gradual due to the averaging-effect between individuals of different species and sizes. This is illustrated in Figure 3 where the Caxiuana traces have a gradual transition due to the higher standard deviation of the midday water potential data (based on 161 trees from 36 species in the Brazilian Amazon (Bittencourt et al. 2020)) than in other sites. On the other hand, soil contains such a high proportion of the water in ecosystems (Figures 1 and S3.1), that community-level transitions could be driven by the shape of the soil water release curve (Asgarzadeh et al. 2014; Dexter, Czyz, and Richard 2012; Wood et al. 2023). The degree of coordination

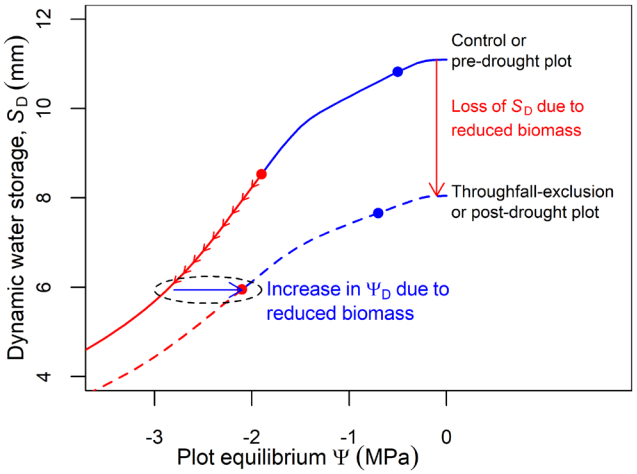

FIGURE 6 | A comparison of the dynamic water storage (sapwood and canopy) and plot equilibrium water potential of the drought plot (thick dashed line) and control plot (thick solid line) in the Caxiuana throughfall-exclusion experiment, based on data presented in Figure 3. The red and blue points on each thick line represent the threshold water potential and measured predawn water potentials, respectively. The blue section of each line indicates the amount of water available in each plot for 'reversible' changes in ecosystem water content, i.e., changes that do not cause physiological damage. The red section of each of the thick lines represent a trajectory of water loss resulting in physiological damage and loss of living tissue/functional biomass. We hypothesise that the transition of the drought plot into its current reduced biomass state followed the red arrows to the point at which the biomass reached its current value given the available water. At that point, the equilibrium water potential would have returned to within the normal physiological range represented by the blue arrow (highlighted by the ellipse).

in PV relationships between vegetation and soil requires further investigation.

4.2 | Modelling Applications

The trend in the water: biomass ratio (Figure 5e,f) and the lack of systematic change in the relative capacitance across sites, provides a starting point for addressing the question of whether we can model ecosystems as structures that self-organise to achieve a steady state with respect to longer-term environmental pressures. This approach is complementary but distinct from the process-based approach (Fisher et al. 2018) by having lower resolution data requirements, requiring only information on 'states' (Ψ and θ), which are more feasibly sampled and interpolated across larger areas, and reducing the dependence on characterising the highly dynamic flux responses and variation across trees, species, size classes and functional types. Our ability to link climate with large-scale trends in vegetation properties will continue to increase with the growth of global databases on plant traits (Mencuccini et al. 2019) and water potentials (Novick et al. 2022), coupled with the increased capacity to estimate water content at large scales (Konings et al. 2021). Water is more directly linked to climate and land surface energy budgets than is carbon (Bonan 2008; Malhi et al. 2002; Tesař et al. 2007). Thus, in a process analogous to modelling water levels in a lake, the state-based approach may offer an alternative method for making long-term predictions of climate-related changes in vegetation structure in terms of biomass, leaf area and allometry.

4.3 | Temporal and Spatial Resolution

How relevant are changes in equilibrium water potential to vegetation structure and function? Across the nine sites in this study, a complete loss of leaf area would result in a median of < 5% decrease in the dynamic storage fraction, S_D. Leaf turgor loss point is typically around 80%–90% relative water content (Bartlett, Scoffoni, and Sack 2012; Martinez-Vilalta et al. 2019), suggesting daily variations in leaf water storage, S_{leaves}, of only 10%–20% of the thickness of the solid lines in Figures 3 and 4, i.e., a small fraction of the accessible storage. The change in water status of this small fraction of the system determines sub-daily rates of water and carbon fluxes, which therefore cannot be estimated using equilibrium water potential.

Systems are most dynamic, however, when they are least water stressed, i.e., the less negative predawn water potentials are, the greater the difference between predawn and midday water potentials can be. In contrast to what may occur at tissue-level, a system-level threshold is only likely to be crossed when at, or close to, equilibrium water potentials (Figure 1c). Therefore, while equilibrium water potentials do not capture sub-daily variation in fluxes, the state-based approach does capture changes in water status over the longer term which are likely to relate more directly to climate-related changes in biomass (Bauman et al. 2022).

4.4 | Remote Sensing Applications

The VOD signal from satellite microwave remote sensing is most sensitive to upper canopy dynamics, while the timing of satellite VOD measurements is predetermined by overpass times making it difficult to 'select' equilibrium/predawn conditions. Consequently, the degree to which VOD relates to the EPV curves is dependent on the frequency of the signal where e.g., X-band may only detect canopy dynamics, while L- (and lower frequency) bands may relate more to the total amount of water in the system and equilibrium water potentials.

Because the penetration depth of the VOD signal is not known, it is currently difficult to relate VOD to an absolute quantity of water. However, understanding generalised relationships between water relations and biomass potentially leads to a better understanding of plant water relations at the relevant spatial scale. The evidence suggesting that (i) maximum vegetation water content varies predictably with biomass, and that (ii) relative accessible water storage does not appear to differ systematically between systems (Figure 5), provide a starting point for inferring ecosystem water status from remote sensing data. Nevertheless, additional research is needed to account for the varying sensitivity of the remote sensing data to canopy water content across different depth layers (Holtzman et al. 2021), and what observation times and other conditions would be most closely related to the equilibrium conditions described in this study.

4.5 | Ecological Sampling Strategies—Species Versus Landscape

The state-based approach uses 'vegetation' as the functional unit, rather than species, functional types, or individuals, thereby differing from the trait-based information that typically informs process-based models. The assumption is that the emergent structure of natural communities is more predictable than the abundance or trajectory of any given species or functional type, and therefore, that climate-mediated changes in vegetation structure could be predicted in the absence of species-level or trait information. An open question is whether our data collection practices have led to an accurate representation of vegetation as a functional unit, rather than of individual species functioning in isolation.

Field studies tend to collect data that represents the most stressed part of the system (e.g., midday leaf water potentials in upper canopy sunlit leaves (Martínez-Vilalta and Garcia-Forner 2017)) and traits of dominant species (e.g., vulnerability thresholds). While such data are well-suited to predicting relatively short-term stress responses of ecosystems, they may be less informative of longer-term transitions and fail to capture possible steady-state ecosystem-climate interactions. One limitation is that, under given conditions, the physical location and size of an individual may account for greater differences in state variables (e.g., water potential, stomatal conductance) than species-level traits (Meinzer, Goldstein, and Andrade 2001). An additional limitation is that the characteristics of a tissue sample may not represent the organism; where hydraulic measurements are principally taken on leaves and small twigs which can be expendable at the organism-level—as indicated by self-pruning and non-fatal canopy die-back (Zimmermann 1983).

To capture responses of ecosystems over longer time scales, it may be necessary to characterise the distribution of state variables across individuals and through space (horizontally and vertically), rather than just the extreme values. The distribution of water potential within a community arises as a function of the traits, species and the feedbacks between community structure and the boundary layer conditions. Therefore, randomised spatial sampling, or systematic point sampling over a grid or transect, may be more suitable for representing ecosystem properties, relating more directly to landscape-level feedbacks between vegetation, climate and biogeochemical cycles. Systematic sampling of the landscape may therefore reveal trends and commonalities between taxonomically distinct but climatically and functionally similar systems, while potentially being more practical for characterising highly biodiverse communities.

4.6 | Further Considerations

Vegetation predawn water potentials are commonly not in equilibrium with the root water source owing to nocturnal fluxes such as transpiration (Donovan, Richards, and Linton 2003; Kangur et al. 2021) or foliar water uptake (Binks et al. 2019; Kangur, Kupper, and Sellin 2017). The effect of wrongly assuming plants are in equilibrium with the soil is typically in assuming that they are in equilibrium with a different part of the soil profile. If the nocturnal flux is small, it seems likely that the disequilibrium soil depth is also small (Kangur, Kupper, and Sellin 2017).

We used an empirical relationship between wood density and the saturated water content of sapwood to calculate S when $\Psi = 0$. There is a known 'plateaux effect' in leaves, wood and porous media in general, where pore spaces that would be empty at very small negative water potentials become full of water. This effect has not been accounted for in the *Proof of concept* due to the difficulty in characterising it at whole tree scale and given the uncertainty in the other parameters. The plateaux effect may have resulted in an overestimation of the total water content at $\Psi = 0$, although this error is likely to be small in comparison with the uncertainty surrounding the heartwood contribution.

5 | Summary

The ecosystem-scale PV curve reconciles our detailed and physically rigorous understanding of small-scale field-measurable processes to the spatial scale applicable to ecosystem and climate science. The 'state-based' approach to understanding climate-vegetation feedbacks is based on the principle that ecosystems reach a thermodynamic steady state with respect to environmental conditions. This assumption allows us to use data with low temporal resolution, thereby determining long-term changes in stores of carbon and water and becoming less dependent on the measurement of processes with high spatial and temporal variability. Acknowledging the existence of additional constraints (e.g., soil nutrients), we propose that to a first approximation the water content and biomass of an ecosystem is a direct function of the hydraulic environment, that is, the water potential of the soil and the atmosphere.

We conclude that using the water content of the leaves and above ground sapwood, the dynamic fraction, and water potentials during equilibrium (e.g., predawn or drought) conditions, are practical options for calculating baseline ecosystem PV parameters. This is based on (i) the practicality of applying an equilibrium concept to a non-equilibrium system, (ii) the relevance of these parameters in relating large-scale vegetation function to the hydraulic environment and (iii) the availability of existing data. Derivations of both water potential and storage (Ψ_{AGB} and S_{AGB}) could be improved from our estimates with more comprehensive data on water potential, water content and capacitance at larger scale and better spatial representation across landscapes.

Our first estimates here, for a range of ecosystems, suggest that there appears to be a consistent ratio of 'dynamic', or physiologically active, water to biomass across the examined plots of approximately 1:3. In absolute terms, the water available for reversible changes in S_D, and hydraulic capacitance, also increases with biomass. In relative terms, there were no significant relationships between water relations properties and biomass, possibly suggesting these relative values are conserved across ecosystems. Such generalisations across biomes offer the first insight into the utility of the state-based approach for gaining

ecophysiologically meaningful interpretations of landscape-scale data and provide a robust basis for the interpretation of remote sensing VOD observations.

Author Contributions

Oliver Binks: conceptualization, data curation, formal analysis, funding acquisition, investigation, methodology, project administration, resources, software, validation, visualization, writing – original draft, writing – review and editing. **Patrick Meir:** conceptualization, funding acquisition, resources, supervision, writing – review and editing. **Alexandra G. Konings:** conceptualization, visualization, writing – review and editing. **Lucas Cernusak:** data curation. **Bradley O. Christoffersen:** conceptualization, validation, visualization, writing – review and editing. **William R. L. Anderegg:** writing – review and editing. **Jeffrey Wood:** writing – review and editing. **Lawren Sack:** conceptualization, validation, visualization, writing – review and editing. **Jordi Martinez-Vilalta:** conceptualization, methodology, validation, visualization, writing – review and editing. **Maurizio Mencuccini:** conceptualization, funding acquisition, resources, supervision, validation, visualization, writing – review and editing.

Acknowledgements

This work was partially inspired by discussions at the "Sensing Forest Water Dynamics from Space: Towards Predicting the Earth System Response to Droughts" workshop, which was initiated and supported by the W.M. Keck Institute for Space Studies.

Catalan science and technology grant, Beatriu de Pinós, BP2021 00224 and 'la Caixa' Junior Leader Fellowship LCF/BQ/PI23/11970013 to OB; EU Horizon 2020 grant 862221 to MM; ARC grant DP17010409, NERC NE/W006308/1 and Royal Society RSWF\211008 to PM.

Conflicts of Interest

The authors declare no conflicts of interest.

Data Availability Statement

Data will be made available in public repositories on acceptance of the article. For review purposes the data, metadata, code and a readme file are temporarily available from: https://doi.org/10.5061/dryad.qrfj6q5p7

References

Ambaum, M. H. P. 2020. "Accurate, Simple Equation for Saturated Vapour Pressure Over Water and Ice." *Quarterly Journal of the Royal Meteorological Society* 146, no. 733: 4252–4258. https://doi.org/10.1002/qj.3899.

Anderegg, W. R. L., L. D. L. Anderegg, and C. Huang. 2019. "Testing Early Warning Metrics for Drought-Induced Tree Physiological Stress and Mortality." *Global Change Biology* 25, no. 7: 2459–2469. https://doi.org/10.1111/gcb.14655.

Andrade, P., R. M. Lemus, and C. Pérez. 2011. "Models of Sorption Isotherms for Food: Uses and Limitations." *Vitae* 18, no. 3: 325–334. http://www.scielo.org.co/scielo.php?script=sci_arttext&pid=S0121-40042011000300012&lng=en&nrm=iso&tlng=en.

Aparecido, L. M. T., G. R. Miller, A. T. Cahill, and G. W. Moore. 2016. "Comparison of Tree Transpiration Under Wet and Dry Canopy Conditions in a Costa Rican Premontane Tropical Forest." *Hydrological Processes* 5011: 5000–5011. https://doi.org/10.1002/hyp.10960.

Aritsara, A. N. A., S. Wang, B.-N. Li, et al. 2022. "Divergent Leaf and Fine Root "Pressure–Volume Relationships" Across Habitats With Varying Water Availability." *Plant Physiology* 190, no. 4: 2246–2259. https://doi.org/10.1093/PLPHYS/KIAC403.

Asgarzadeh, H., M. R. Mosaddeghi, A. R. Dexter, A. A. Mahboubi, and M. R. Neyshabouri. 2014. "Determination of Soil Available Water for Plants: Consistency Between Laboratory and Field Measurements." *Geoderma* 226–227, no. 1: 8–20. https://doi.org/10.1016/J.GEODERMA.2014.02.020.

Bartlett, M. K., C. Scoffoni, and L. Sack. 2012. "The Determinants of Leaf Turgor Loss Point and Prediction of Drought Tolerance of Species and Biomes: A Global Meta-Analysis." *Ecology Letters* 15, no. 5: 393–405. https://doi.org/10.1111/j.1461-0248.2012.01751.x.

Bartlett, M. K., G. Sinclair, G. Fontanesi, T. Knipfer, M. A. Walker, and A. J. McElrone. 2022. "Root Pressure–Volume Curve Traits Capture Rootstock Drought Tolerance." *Annals of Botany* 129, no. 4: 389–402. https://doi.org/10.1093/AOB/MCAB132.

Bauman, D., C. Fortunel, G. Delhaye, et al. 2022. "Tropical Tree Mortality Has Increased With Rising Atmospheric Water Stress." *Nature* 608: 528–533. https://doi.org/10.1038/s41586-022-04737-7.

Beringer, J., L. B. Hutley, I. McHugh, et al. 2016. "An Introduction to the Australian and New Zealand Flux Tower Network—OzFlux." *Biogeosciences* 13, no. 21: 5895–5916. https://doi.org/10.5194/BG-13-5895-2016.

Binks, O., L. A. Cernusak, M. Liddell, et al. 2023. "Vapour Pressure Deficit Modulates Hydraulic Function and Structure of Tropical Rainforests Under Nonlimiting Soil Water Supply." *New Phytologist* 240: 1405–1420. https://doi.org/10.1111/NPH.19257.

Binks, O., L. A. Cernusak, M. Liddell, et al. 2021. "Forest System Hydraulic Conductance: Partitioning Tree and Soil Components." *New Phytologist* 233, no. 4: 1667–1681. https://doi.org/10.1111/nph.17895.

Binks, O., P. Meir, A. G. Konings, et al. 2024. "Data from: A theoretical framework to quantify ecosystem pressure-volume relationships." Dryad. http://datadryad.org/stash/share/IYvv_nGYhIYBgy6OiZb2Aj6VcAk-LPz-UQI235M_gbf8 DOI: https://doi.org/10.5061/dryad.qrfj6q5p7.

Binks, O., P. Meir, L. Rowland, et al. 2016. "Plasticity in Leaf-Level Water Relations of Tropical Rainforest Trees in Response to Experimental Drought." *New Phytologist* 211, no. 2: 477–488. https://doi.org/10.1111/nph.13927.

Binks, O., M. Mencuccini, L. Rowland, et al. 2019. "Foliar Water Uptake in Amazonian Trees: Evidence and Consequences." *Global Change Biology* 25, no. 8: 1–13. https://doi.org/10.1111/gcb.14666.

Bittencourt, P. R. L., R. S. Oliveira, A. C. L. da Costa, et al. 2020. "Amazonia Trees Have Limited Capacity to Acclimate Plant Hydraulic Properties in Response to Long-Term Drought." *Global Change Biology* 26, no. 6: 3569–3584. https://doi.org/10.1111/gcb.15040.

Bonan, G. B. 2008. "Forests and Climate Change: Forcings, Feedbacks, and the Climate Benefits of Forests." *Science* 320, no. 5882: 1444–1449. https://doi.org/10.1126/science.1155121.

Brandt, M., J. P. Wigneron, J. Chave, et al. 2018. "Satellite Passive Microwaves Reveal Recent Climate-Induced Carbon Losses in African Drylands." *Nature Ecology & Evolution* 2, no. 5: 827–835. https://doi.org/10.1038/s41559-018-0530-6.

Brodribb, T. J., and N. M. Holbrook. 2003. "Stomatal Closure During Leaf Dehydration, Correlation With Other Leaf Physiological Traits 1." *Plant Physiology* 132: 2166–2173. https://doi.org/10.1104/pp.103.023879.sensitive.

Brooks, R. H. H., and A. T. T. Corey. 1964. "Hydraulic Properties of Porous Media." *Physics and Chemistry of Glasses: European Journal of Glass Science and Technology Part B* 49, no. 6: 293–296. citeulike-article-id:711012.

Cabon, A., J. Martínez-Vilalta, J. Martínez de Aragón, R. Poyatos, and M. de Cáceres. 2018. "Applying the Eco-Hydrological Equilibrium Hypothesis to Model Root Distribution in Water-Limited Forests." *Ecohydrology* 11, no. 7: e2015. https://doi.org/10.1002/ECO.2015.

Carrasco, L. O., S. J. Bucci, D. di Francescantonio, et al. 2015. "Water Storage Dynamics in the Main Stem of Subtropical Tree Species Differing in Wood Density, Growth Rate and Life History Traits." *Tree Physiology* 35, no. 4: 354–365. https://doi.org/10.1093/treephys/tpu087.

Čermák, J., J. Kucera, W. L. Bauerle, N. Phillips, and T. M. Hinckley. 2007. "Tree Water Storage and Its Diurnal Dynamics Related to Sap Flow and Changes in Stem Volume in Old-Growth Douglas-Fir Trees." *Tree Physiology* 27, no. 2: 181–198. https://doi.org/10.1093/treephys/27.2.181.

Christoffersen, B. O., M. Gloor, S. Fauset, et al. 2016. "Linking Hydraulic Traits to Tropical Forest Function in a Size-Structured and Trait-Driven Model (TFS v.1-Hydro)." *Geoscientific Model Development* 9, no. 11: 4227–4255. https://doi.org/10.5194/gmd-9-4227-2016.

Cordero, L. D. P., and M. Kanninen. 2003. "Heartwood, Sapwood and Bark Content, and Wood Dry Density of Young and Mature Teak (Tectona Grandis) Trees Grown in Costa Rica." *Silva Fennica* 37, no. 1: 45–54. https://doi.org/10.14214/sf.511.

da Costa, A. C. L., D. Galbraith, S. Almeida, et al. 2010. "Effect of 7 Yr of Experimental Drought on Vegetation Dynamics and Biomass Storage of an Eastern Amazonian Rainforest." *New Phytologist* 187, no. 3: 579–591. https://doi.org/10.1111/j.1469-8137.2010.03309.x.

Dewar, R. C., O. Franklin, A. Makela, R. E. Mcmurtrie, and H. T. Valentine. 2009. "Optimal Function Explains Forest Responses to Global Change." *Bioscience* 59, no. 2: 127–139. https://doi.org/10.1525/bio.2009.59.2.6.

Dexter, A. R., E. A. Czyz, and G. Richard. 2012. "Equilibrium, Non-equilibrium and Residual Water: Consequences for Soil Water Retention." *Geoderma* 177–178: 63–71. https://doi.org/10.1016/J.GEODERMA.2012.01.029.

Dlouhá, J., T. Alméras, J. Beauchêne, B. Clair, and M. Fournier. 2018. "Biophysical Dependences Among Functional Wood Traits." *Functional Ecology* 32, no. 12: 2652–2665. https://doi.org/10.1111/1365-2435.13209.

Donovan, L. A., J. H. Richards, and M. J. Linton. 2003. "Magnitude and Mechanisms of Disequilibrium Between Predawn Plant and Soil Water Potentials." *Ecology* 84, no. 2: 463–470.

Eagleson, P. 1982. "Ecological Optimality in Water-Limited Natural Soil-Vegetation Systems 1. Theory and Hypothesis." *Water Resources Research* 18, no. 2: 325–340.

Faiz, S. M. A., and P. E. Weatherley. 1982. "Root Contraction in Transpiring Plants." *New Phytologist* 92, no. 3: 333–343. https://doi.org/10.1111/j.1469-8137.1982.tb03391.x.

Fisher, R. A., C. D. Koven, W. R. L. Anderegg, et al. 2018. "Vegetation Demographics in Earth System Models: A Review of Progress and Priorities." *Global Change Biology* 24, no. 1: 35–54. https://doi.org/10.1111/gcb.13910.

Fisher, R. A., M. Williams, R. L. Do Vale, et al. 2006. "Evidence From Amazonian Forests Is Consistent With Isohydric Control of Leaf Water Potential." *Plant, Cell & Environment* 29, no. 2: 151–165. http://www.ncbi.nlm.nih.gov/pubmed/17080631.

Franklin, O., S. P. Harrison, R. Dewar, et al. 2020. "Organizing Principles for Vegetation Dynamics." *Nature Plants* 6, no. 5: 444–453. https://doi.org/10.1038/s41477-020-0655-x.

Franzen, C., and P. W. Mirwald. 2004. "Moisture Content of Natural Stone: Static and Dynamic Equilibrium With Atmospheric Humidity." *Environmental Geology* 46, no. 3–4: 391–401. https://doi.org/10.1007/S00254-004-1040-1.

Frappart, F., J.-P. Wigneron, X. Li, et al. 2020. "Global Monitoring of the Vegetation Dynamics from the Vegetation Optical Depth (VOD): A Review." *Remote Sensing* 12: 2915. https://doi.org/10.3390/rs12182915.

Gartner, B. L., ed. 1995. *Plantstems: Physiology and Functional Morphology*. San Diego, CA: Academic Press.

Gibbs, J. W. 1873. "Graphical Methods in the Thermodynamics of Fluids." *Transactions of the Connecticut Academy* 2: 309–342.

Glass, S. V., and S. L. Zelinka. 2010. "Physical Properties and Moisture Relations of Wood." *Wood Handbook; Wood as an Engineering Material* 113: 3.1. https://www.fs.usda.gov/treesearch/pubs/7150.

Hartmann, H., C. F. Moura, W. R. L. Anderegg, et al. 2018. "Research Frontiers for Improving Our Understanding of Drought-Induced Tree and Forest Mortality." *New Phytologist* 218, no. 1: 15–28. https://doi.org/10.1111/nph.15048.

Henry, C., G. P. John, R. Pan, et al. 2019. "A Stomatal Safety-Efficiency Trade-Off Constrains Responses to Leaf Dehydration." *Nature Communications* 10, no. 1: 1–9. https://doi.org/10.1038/s41467-019-11006-1.

Hillel, D. 1977. *Environmental Soil Physics*. 1st ed, 771. San Diego, California: Academic Press. https://www.elsevier.com/books/environmental-soil-physics/hillel/978-0-12-348525-0.

Holdridge, L. R. 1947. "Determination of World Plant Formations From Simple Climatic Data." *Science* 105, no. 2727: 367–368. https://doi.org/10.1126/SCIENCE.105.2727.367/ASSET/D5F5223D-A362-48CE-A019-A6BD2BD268B4/ASSETS/SCIENCE.105.2727.367.FP.PNG.

Hollander, E. H. D. 1979. "Estimation of the Pore Size Distribution From the Moisture Characteristic." *Water Resources Research* 15, no. 1: 107.

Hölttä, T., H. Cochard, E. Nikinmaa, and M. Mencuccini. 2009. "Capacitive Effect of Cavitation in Xylem Conduits: Results From a Dynamic Model." *Plant, Cell and Environment* 32, no. 1: 10–21. https://doi.org/10.1111/j.1365-3040.2008.01894.x.

Holtzman, N. M., L. D. L. Anderegg, S. Kraatz, et al. 2021. "L-Band Vegetation Optical Depth as an Indicator of Plant Water Potential in a Temperate Deciduous Forest Stand." *Biogeosciences* 18, no. 2: 739–753. https://doi.org/10.5194/BG-18-739-2021.

Humboldt, A. von., and A. Bonpland. 1805. Essai sur la géographie des plantes: accompagné d'un tableau physique des régions équinoxiales, fondé sur des mesures exécutées, depuis le dixième degré de latitude boréale jusqu'au dixième degré de latitude australe, pendant les années 1799, 1800, 1801, 1802 et 1803. Chez Levrault, Schoell et compagnie, libraires. https://www.biodiversitylibrary.org/item/37872.

Jackson, T. J., and T. J. Schmugge. 1991. "Vegetation Effects on the Microwave Emission of Soils." *Remote Sensing of Environment* 36, no. 3: 203–212. https://doi.org/10.1016/0034-4257(91)90057-D.

Kangur, O., P. Kupper, and A. Sellin. 2017. "Predawn Disequilibrium Between Soil and Plant Water Potentials in Light of Climate Trends Predicted for Northern Europe." *Regional Environmental Change* 17, no. 7: 2159–2168. https://doi.org/10.1007/s10113-017-1183-8.

Kangur, O., K. Steppe, J. D. M. Schreel, J. S. Von Der Crone, and A. Sellin. 2021. "Variation in Nocturnal Stomatal Conductance and Development of Predawn Disequilibrium Between Soil and Leaf Water Potentials in Nine Temperate Deciduous Tree Species." *Functional Plant Biology* 48, no. 5: 483–492. https://doi.org/10.1071/FP20091.

Kleidon, A., Y. Malhi, and P. M. Cox. 2010. "Maximum Entropy Production in Environmental and Ecological Systems." *Philosophical Transactions of the Royal Society, B: Biological Sciences* 365, no. 1545: 1297–1302. https://doi.org/10.1098/rstb.2010.0018.

Kleidon, A., and S. Schymanski. 2008. "Thermodynamics and Optimality of the Water Budget on Land: A Review." *Geophysical Research Letters* 35, no. 20: 1–6. https://doi.org/10.1029/2008GL035393.

Knapic, S., F. Tavares, and H. Pereira. 2006. "Heartwood and Sapwood Variation in Acacia Melanoxylon R. Br. Trees in Portugal." *Forestry* 79, no. 4: 371–380. https://doi.org/10.1093/forestry/cpl010.

Konings, A. G., X. Feng, A. Molini, S. Manzoni, G. Vico, and A. Porporato. 2012. "Thermodynamics of an Idealized Hydrologic Cycle." *Water Resources Research* 48, no. 5: 1–13. https://doi.org/10.1029/2011WR011264.

Konings, A. G., M. Piles, K. Rötzer, K. A. McColl, S. K. Chan, and D. Entekhabi. 2016. "Vegetation Optical Depth and Scattering Albedo Retrieval Using Time Series of Dual-Polarized L-Band Radiometer Observations." *Remote Sensing of Environment* 172: 178–189. https://doi.org/10.1016/j.rse.2015.11.009.

Konings, A. G., K. Rao, and S. C. Steele-Dunne. 2019. "Macro to Micro: Microwave Remote Sensing of Plant Water Content for Physiology and Ecology." *New Phytologist* 223, no. 3: 1166–1172. https://doi.org/10.1111/nph.15808.

Konings, A. G., S. S. Saatchi, C. Frankenberg, et al. 2021. "Detecting Forest Response to Droughts With Global Observations of Vegetation Water Content." *Global Change Biology* 27: 1–20. https://doi.org/10.1111/gcb.15872.

Koubaa, A., P. Perré, R. Hutcheon, and J. Lessard. 2008. "Complex Dielectric Properties of the Sapwood of Aspen, White Birch, Yellow Birch, and Sugar Maple." *Drying Technology* 26, no. 5: 568–578. https://doi.org/10.1080/07373930801944762.

Kunert, N., L. M. T. Aparecido, S. Wolff, et al. 2017. "A Revised Hydrological Model for the Central Amazon: The Importance of Emergent Canopy Trees in the Forest Water Budget." *Agricultural and Forest Meteorology* 239: 47–57. https://doi.org/10.1016/j.agrformet.2017.03.002.

Malhi, Y., E. Pegoraro, A. D. Nobre, et al. 2002. "Energy and Water Dynamics of a Central Amazonian Rain Forest." *Journal of Geophysical Research-Atmospheres* 107, no. 20: 1–17. https://doi.org/10.1029/2001JD000623.

Mallick, K., I. Trebs, E. Boegh, et al. 2016. "Canopy-Scale Biophysical Controls of Transpiration and Evaporation in the Amazon Basin, Hydrol." *Earth System Science* 20: 4237–4264. https://doi.org/10.5194/hess-20-4237-2016.

Martinez-Vilalta, J., W. R. L. Anderegg, G. Sapes, and A. Sala. 2019. "Greater Focus on Water Pools May Improve Our Ability to Understand and Anticipate Drought-Induced Mortality in Plants." *New Phytologist* 223, no. 1: 22–32. https://doi.org/10.1111/nph.15644.

Martínez-Vilalta, J., and N. Garcia-Forner. 2017. "Water Potential Regulation, Stomatal Behaviour and Hydraulic Transport Under Drought: Deconstructing the Iso / Anisohydric Concept." *Plant, Cell & Environment* 40, no. 6: 962–976. https://doi.org/10.1111/pce.12846.

Mavrovic, A., A. Roy, A. Royer, et al. 2018. "Dielectric Characterization of Vegetation at L Band Using an Open-Ended Coaxial Probe." *Geoscientific Instrumentation, Methods and Data Systems* 7, no. 3: 195–208. https://doi.org/10.5194/gi-7-195-2018.

Mc Naught, A. D., and A. Wilkinson. 1997. *IUPAC. Compendium of Chemical Terminology, (the "Gold Book").* 2nd ed. Oxford: Blackwell Scientific Publications Online version (2019-) created by S. J. Chalk. ISBN 0-9678550-9-8. https://doi.org/10.1351/goldbook.

Mcculloh, K. A., D. M. Johnson, F. C. Meinzer, and D. R. Woodruff. 2014. "The Dynamic Pipeline: Hydraulic Capacitance and Xylem Hydraulic Safety in Four Tall Conifer Species." *Plant, Cell & Environment* 37, no. 5: 1171–1183. https://doi.org/10.1111/pce.12225.

McDowell, N. G., G. Sapes, A. Pivovaroff, et al. 2022. "Mechanisms of Woody-Plant Mortality Under Rising Drought, CO_2 and Vapour Pressure Deficit." *Nature Reviews Earth and Environment* 3, no. 5: 294–308. https://doi.org/10.1038/s43017-022-00272-1.

Meinzer, F. C., G. Goldstein, and J. L. Andrade. 2001. "Regulation of Water Flux Through Tropical Forest Canopy Trees: Do Universal Rules Apply?" *Tree Physiology* 21, no. 1: 19–26. https://doi.org/10.1093/TREEPHYS/21.1.19.

Meinzer, F. C., S. A. James, G. Goldstein, and D. Woodruff. 2003. "Whole-Tree Water Transport Scales With Sapwood Capacitance in Tropical Forest Canopy Trees." *Plant, Cell and Environment* 26, no. 7: 1147–1155. https://doi.org/10.1046/j.1365-3040.2003.01039.x.

Meir, P., P. Meir, M. Mencuccini, and R. C. Dewar. 2015. "Drought-Related Tree Mortality: Addressing the Gaps in Understanding and Prediction." *New Phytologist* 207, no. 1: 28–33. https://doi.org/10.1111/nph.13382.

Meir, P., M. Mencuccini, O. Binks, A. L. da Costa, L. Ferreira, and L. Rowland. 2018. "Short-Term Effects of Drought on Tropical Forest Do Not Fully Predict Impacts of Repeated or Long-Term Drought: Gas Exchange Versus Growth." *Philosophical Transactions of the Royal Society, B: Biological Sciences* 373, no. 1760: 20170311. https://doi.org/10.1098/rstb.2017.0311.

Mencuccini, M., T. Rosas, L. Rowland, et al. 2019. "Leaf Economics and Plant Hydraulics Drive Leaf: Wood Area Ratios." *New Phytologist* 224, no. 4: 1544–1556. https://doi.org/10.1111/nph.15998.

Moore, G. W., G. Orozco, L. M. T. Aparecido, and G. R. Miller. 2017. "Upscaling Transpiration in Diverse Forests: Insights From a Tropical Premontane Site." *Ecohydrology* 11, no. 3: 1–13. https://doi.org/10.1002/eco.1920.

Nobel, P. S. 2009. *Physicochemical and Environmental Plant Physiology.* San Diego, California: Academic Press. https://doi.org/10.1016/B978-0-12-374143-1.X0001-4.

Novick, K. A., D. L. Ficklin, D. Baldocchi, et al. 2022. "Confronting the Water Potential Information Gap." *Nature Geoscience* 15, no. 3: 158–164. https://doi.org/10.1038/s41561-022-00909-2.

ORNL DAAC. 2018. *MODIS and VIIRS Land Products Global Subsetting and Visualization Tool*. Oak Ridge, TN, USA: ORNL DAAC. https://doi.org/10.3334/ORNLDAAC/1379.

Peters, J. M. R., R. López, M. Nolf, et al. 2021. "Living on the Edge: A Continental-Scale Assessment of Forest Vulnerability to Drought." *Global Change Biology* 27, no. 15: 3620–3641. https://doi.org/10.1111/gcb.15641.

Pickard, W. F. 1981. "The Ascent Of sap In Plants." *Progress in Biophysics & Molecular biology* 37, no. 3: 181–229.

Rao, S. M., and M. Rekapalli. 2020. "Identifying the Dominant Mode of Moisture Transport During Drying of Unsaturated Soils." *Scientific Reports* 10, no. 1: 1–9. https://doi.org/10.1038/s41598-020-61302-w.

Rodriguez-Dominguez, C. M., and T. J. Brodribb. 2020. "Declining Root Water Transport Drives Stomatal Closure in Olive Under Moderate Water Stress." *New Phytologist* 225, no. 1: 126–134. https://doi.org/10.1111/nph.16177.

Rosner, S., B. Heinze, and T. Savi. 2019. "Prediction of Hydraulic Conductivity Loss from Relative Water loss: New Insights Into Water Storage of Tree Stems and Branches." *Physiologia Plantarum* 165, 843–854. https://doi.org/10.1111/ppl.12790.

Ruel, J. J., and M. P. Ayres. 1999. "Jensen's Inequality Predicts Effects of Environmental Variation." *Trends in Ecology & Evolution* 14, no. 9: 361–366. https://doi.org/10.1016/S0169-5347(99)01664-X.

Sanchez-Martinez, P., J. Martínez-Vilalta, K. G. Dexter, R. A. Segovia, and M. Mencuccini. 2020. "Adaptation and Coordinated Evolution of Plant Hydraulic Traits." *Ecology Letters* 23, no. 11: 1599–1610. https://doi.org/10.1111/ele.13584.

Scholz, F. G., S. J. Bucci, G. Goldstein, F. C. Meinzer, A. C. Franco, and F. Miralles-Wilhelm. 2007. "Biophysical Properties and Functional Significance of Stem Water Storage Tissues in Neotropical Savanna Trees." *Plant, Cell and Environment* 30, no. 2: 236–248. https://doi.org/10.1111/j.1365-3040.2006.01623.x.

Schönbeck, L., A. Gessler, G. Hoch, et al. 2018. "Homeostatic Levels of Nonstructural Carbohydrates After 13 Yr. of Drought and Irrigation in Pinus Sylvestris." *New Phytologist* 219, no. 4: 1314–1324. https://doi.org/10.1111/nph.15224.

Sperry, J. S., V. Stiller, and U. G. Hacke. 2003. "Xylem Hydraulics and the Soil–Plant–Atmosphere Continuum: Opportunities and Unresolved

Issues." *Agronomy Journal* 95, no. 6: 1362–1370. https://doi.org/10.2134/AGRONJ2003.1362.

Sperry, J. S., M. D. Venturas, H. N. Todd, et al. 2019. "The Impact of Rising CO_2 and Acclimation on the Response of US Forests to Global Warming." *Proceedings of the National Academy of Sciences of the United States of America* 116: 25,734–25,744. https://doi.org/10.6084/m9.figshare.8805110.

Steudle, E. 2000. "Water Uptake by Roots: Effects of Water Deficit." *Journal of Experimental Botany* 51, no. 350: 1531–1542. https://doi.org/10.1093/jexbot/51.350.1531.

Stewart, G. R., C. A. Gracia, E. E. Hegarty, and R. L. Specht. 1990. "Nitrate Reductase Activity and Chlorophyll Content in Sun Leaves of Subtropical Australian Closed-Forest (Rainforest) and Open-Forest Communities." *Oecologia* 82, no. 4: 544–551. https://doi.org/10.1007/BF00319799.

Svennberg, K., and L. Wadsö. 2008. "Sorption Isotherms for Textile Fabrics, Foams and Batting Used in the Indoor Environment." *Journal of the Textile Institute* 99, no. 2: 125–132. https://doi.org/10.1080/00405000701556061.

Tesař, M., M. Šír, Ľ. Lichner, and J. Čermák. 2007. "Plant Transpiration and Net Entropy Exchange on the Earth's Surface in a Czech Watershed." *Biologia* 62, no. 5: 547–551. https://doi.org/10.2478/s11756-007-0108-2.

Tyree, M., and F. Ewers. 1991. "The Hydraulic Architecture of Trees and Other Woody Plants." *New Phytologist* 34: 345–360. https://doi.org/10.1111/j.1469-8137.1991.tb00035.x/abstract.

Tyree, M. T., and H. Hammel. 1972. "The Measurement of the Turgor Pressure and the Water Relations of Plants by the Pressure-Bomb Technique." *Journal of Experimental Botany* 23, no. 74: 267–282. http://jxb.oxfordjournals.org/content/23/1/267.short.

Tyree, M. T., and J. S. Sperry. 1989. "Vulnerability of Xylem to Cavitation and Embolism." *Annual Review of Plant Physiology and Plant Molecular Biology* 40: 19–38.

Ulaby, F., and D. Long. 2014. "Microwave Radar and Radiometric Remote Sensing." In *Microwave Radar and Radiometric Remote Sensing*. Michigan: University of Michigan Press.

Umebayashi, T. 2011. "Green Moisture Content and Basic Density of 95 Woody Species Growing in Kyushu University Forests, Japan."

van der Sande, M. T., P. A. Zuidema, and F. Sterck. 2015. "Explaining Biomass Growth of Tropical Canopy Trees: The Importance of Sapwood." *Oecologia* 177, no. 4: 1145–1155. https://doi.org/10.1007/s00442-015-3220-y.

van Genuchten, M. T. 1980. "A Closed-Form Equation for Predicting the Hydraulic Conductivity of Unsaturated Soils." *Soil Science Society of America Journal* 44, no. 5: 892–898. https://doi.org/10.2136/sssaj1980.03615995004400050002x.

Venturas, M. D., J. S. Sperry, and U. G. Hacke. 2017. "Plant Xylem Hydraulics: What We Understand, Current Research, and Future Challenges." *Journal of Integrative Plant Biology* 59, no. 6: 356–389. https://doi.org/10.1111/jipb.12534.

Wang, X., C. Wang, Q. Zhang, and X. Quan. 2009. "Heartwood and Sapwood Allometry of Seven Chinese Temperate Tree Species." *Annals of Forest Science* 67, no. 4: 410. https://doi.org/10.1051/forest/2009131.

Wolfe, B. T., and T. A. Kursar. 2015. "Diverse Patterns of Stored Water Use Among Saplings in Seasonally Dry Tropical Forests." *Oecologia* 179, no. 4: 925–936. https://doi.org/10.1007/s00442-015-3329-z.

Wood, J. D., L. Gu, P. J. Hanson, C. Frankenberg, and L. Sack. 2023. "The Ecosystem Wilting Point Defines Drought Response and Recovery of a Quercus-Carya Forest." *Global Change Biology* 29: 2015–2029. https://doi.org/10.1111/GCB.16582.

Yang, J., B. E. Medlyn, M. G. de Kauwe, and R. A. Duursma. 2018. "Applying the Concept of Ecohydrological Equilibrium to Predict Steady State Leaf Area Index." *Journal of Advances in Modeling Earth Systems* 10, no. 8: 1740–1758. https://doi.org/10.1029/2017MS001169.

Yao, Y., E. Joetzjer, P. Ciais, et al. 2022. "Forest Fluxes and Mortality Response to Drought: Model Description (ORCHIDEE-CAN-NHA r7236) and Evaluation at the Caxiuanã Drought Experiment." *Geoscientific Model Development* 15, no. 20: 7809–7833. https://doi.org/10.5194/gmd-15-7809-2022.

Zeri, M., L. D. A. Sá, A. O. A. O. Manzi, et al. 2014. "Variability of Carbon and Water Fluxes Following Climate Extremes Over a Tropical Forest in Southwestern Amazonia." *PLoS One* 9, no. 2: e88130. https://doi.org/10.1371/journal.pone.0088130.

Ziemińska, K., E. Rosa, S. M. Gleason, and N. M. Holbrook. 2020. "Wood Day Capacitance Is Related to Water Content, Wood Density, and Anatomy Across 30 Temperate Tree Species." *Plant, Cell & Environment* 43, no. 12: 3048–3067. https://doi.org/10.1111/pce.13891.

Zimmermann, M. H. 1983. *Xylem Structure and the Ascent of Sap / Martin H. Zimmermann*, 1983. Berlin: Springer-Verlag. http://ezproxy.lib.ed.ac.uk/login?url=https://search.ebscohost.com/login.aspx?direct=true&db=cat00234a&AN=edinb.79133&site=eds-live.

Supporting Information

Additional supporting information can be found online in the Supporting Information section.